FAILURE MODE OF STEEL TENSION MEMBERS DUE TO CHANGE IN CONNECTION ECCENTRICITY AND CONNECTION LENGTH

A thesis submitted in partial fulfillment of
the requirement for the award of degree of

MASTER OF ENGINEERING

in

CAD/CAM & ROBOTICS

Submitted By

DIWAKER KUMAR
(80781008)

Under the guidance of

Mr. J. S. SAINI
Sr. Lecturer, Mechanical Engg. Deptt.
Thapar University, Patiala

Mechanical Engineering Department

THAPAR UNIVERSITY PATIALA-147004

JULY, 2009

CERTIFICATE

I hereby declare that the work which is being presented in this thesis entitled, **"FAILURE MODE OF STEEL TENSION MEMBERS DUE TO CHANGE IN CONNECTION ECCENTRICITY AND CONNECTION LENGTH"** in partial fulfillment of requirement for the award of the **MASTER OF ENGINEERING IN CAD/CAM & ROBOTICS** submitted in the **MECHANICAL ENGINEERING DEPARTMENT OF THAPAR UNIVERSITY, PATIALA,** is an authentic record of the initial work carried out by me under the guidance of **Mr. J. S. SAINI, Sr. Lecturer, Mechanical Engineering Department, TU, Patiala** and refers other researcher's works which are duly listed in the references section.

The matter presented in this thesis has not been submitted in part or full to any other university or institute for the award of any degree.

Diwaker Kumar

Dated: 15 July, 09 **(DIWAKER KUMAR)**

This is to certify that above declaration made by the student concerned is correct to the best of my knowledge & belief.

Mr. J. S. SAINI
Sr. Lecturer, MED
Thapar University, Patiala

Countersigned by

Dr. S. K. MOHAPATRA
Professor & Head, MED
Thapar University, Patiala

Dr. R. K. SHARMA
Dean, Academic Affairs
Thapar University, Patiala

ACKNOWLEDGEMENT

Words are often less to revels one's deep regards. With an understanding that work like this can never be the outcome of a single person, I take this opportunity to express my profound sense of gratitude and respect to all those who helped me through the duration of this work.

I am highly grateful to the authorities of Thapar University, Patiala for providing this opportunity to carry out the thesis work.

I would like to express a deep sense of gratitude and thank profusely to my thesis guide **Mr. J. S. SAINI** for their sincere & invaluable guidance, suggestions and attitude which inspired me to submit thesis report in the present form. His feedback and editorial comments were also invaluable for the writing of this thesis. I am thankful to **Dr. S. K. MOHAPATRA,** Prof. & Head**,** Mechanical Engineering Department for providing the facilities for the completion of the work.

At last, I would like to thanks all the members and employees of Mechanical Engineering Department, Thapar University, Patiala for their everlasting support.

Regards,

Diwaker Kumar

(DIWAKER KUMAR)

ABSTRACT

Tension members consisting of single and double angles, single channels and similar sections are frequently used for lateral bracing and as truss elements. Such members normally have eccentric connections which results in bending of tension member. It is often permitted, by current design specifications, to neglect this eccentricity in the design of the member.

The present study is focus on examining the effect of varying connection eccentricity and connection length on the ultimate capacity of the bolted WT tension members. In present study connection length is increased by increasing the pitch between the holes instead of increasing the number of bolts. This work presents six experimental test carried out on WT tension members fastened with bolts, to calculate the failure capacity and also to trace the entire load versus deflection path.

The revolution in computer field has enabled Finite Element Method as major technique for solving engineering design problem with required reliability and accuracy. In present work the Finite Element Analysis of WT section is carried out. The surface-to-surface contact is given between the gusset plate and web of the WT section to fully transfer the load to the web.

Results of Finite Element Analyses are compared with experimental results. The failure capacities predicted by the FEA are in close agreement with the experimental observed failure capacities of the WT section subjected to tensile loading.

NOMENCLATURE

SYMBOLS	DESCRIPTION
P_n	: Normal load
F_y	: Yield strength of material
F_u	: Ultimate strength of material
R_n	: Bolt bearing, bolt shearing or block shear capacities
A_b	: Bolt cross-sectional area
A_g	: Gross cross sectional area
A_e	: Effective net cross-sectional area
A_n	: Net area at cross section
A_{nt}	: Net tension area
A_{gv}	: Gross shear area
A_{gt}	: Gross tension area
A_{nv}	: Net shear area
t_w	: Thickness of web
t_f	: Thickness of flange
U	: Shear lag reduction factor
x	: Connection eccentricity
L	: Connection length
P	: Pitch
d_b	: Bolt diameter

CHAPTER 1
INTRODUCTION

This chapter discusses the basic details and concepts of related topics associated with the thesis work.

1.1 STRUCTURE

Structure is a free-standing, immobile outdoor construction. Typical examples include buildings and non-building structure ones such as bridges and dams. Some structures are temporary, built for some events such as trade shows, conferences or theatre, and often dismantled after use. Temporary structures have fewer constraints relating to future use and durability. Some structures are permanent.

1.2 TRUSS

Truss is a structure, comprising one or more triangular units constructed with straight members whose ends are connected at joints referred to as nodes. External forces and reactions to those forces are considered to act only at the nodes and result in forces in the members which are either tensile or compressive forces. Fig. 1.1 shows the truss.

A planar truss is one where all the members and nodes lie within a two dimensional plane, while a space truss has members and nodes extending into three dimensions.

Fig. 1.1: An example of a truss

1.3 TENSION MEMBER

Tension members are structural elements or members that are subjected to axial tensile forces. Fig. 1.2 shows a member under tension. They are usually used in different types of structures. Examples of tension members are: bracing for buildings and bridges, truss members and cables in suspended roof systems.

In an axially loaded tension member, the stress is given by:

$$F = P / A \tag{1.1}$$

where P is the magnitude of the load and A is the cross-sectional area.

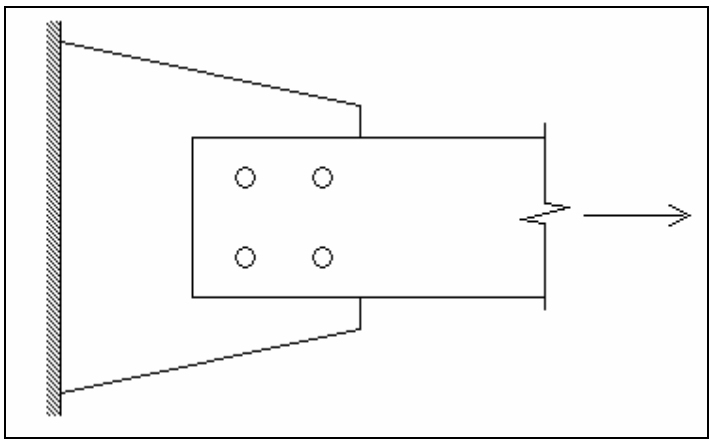

Fig. 1.2: Member under Tension

1.4 DESIGN OF TENSION MEMBER

In order to design tension members, firstly, it is important to analyze how the member would fail under both yielding (excessive deformation) and fracture which considered the limit states. The limit state that produces the smallest design strength is considered the controlling limit state; which also prevent the steel structure from failure. Using AISC (American Institute of Steel Construction), we could obtain the recommended load and resistance factor design approaches.

In the design of a tension member, secondly, it is important to select which type of member and the size of the member is required. The type of member is usually dictated by the location where the member is used. In the case of roof trusses, for

example, angles or pipes are commonly used. Depending upon the span of the truss, the location of the member in the truss and the force in the member either single angle or double angles may be used in roof trusses.

1.5 TENSILE TESTING

The mechanical properties of a material describe the behaviour of material due to physical forces. Mechanical properties occur as a result of the physical properties inherent to each material, and are determined through a series of standardized mechanical tests. One of them is tensile test.

A tensile test, also known as tension test, is probably the most fundamental type of mechanical test performed on material. Tensile tests are simple, relatively inexpensive, and fully standardized. By pulling on something, it can be quickly determined how the material will react to forces being applied in tension. As the material is being pulled, strength can be calculated along with how much it will elongate.

The results of tensile tests are used in selecting materials for engineering applications. Tensile properties frequently are included in material specifications to ensure quality. Tensile properties often are measured during development of new materials and processes, so that different materials and processes can be compared. Finally, tensile properties often are used to predict the behavior of a material under different forms of loading.

Stress-strain curves generated from tensile test results help engineers gain insight into the constitutive relationship between stress and strain for a particular material. The stress-strain curve can also be used to qualitatively describe and classify the material.

Typical regions that can be observed in a stress-strain curve are:

1. Elastic region
2. Yielding
3. Strain Hardening
4. Necking and Failure

These four regions are shown in Fig. 1.3.

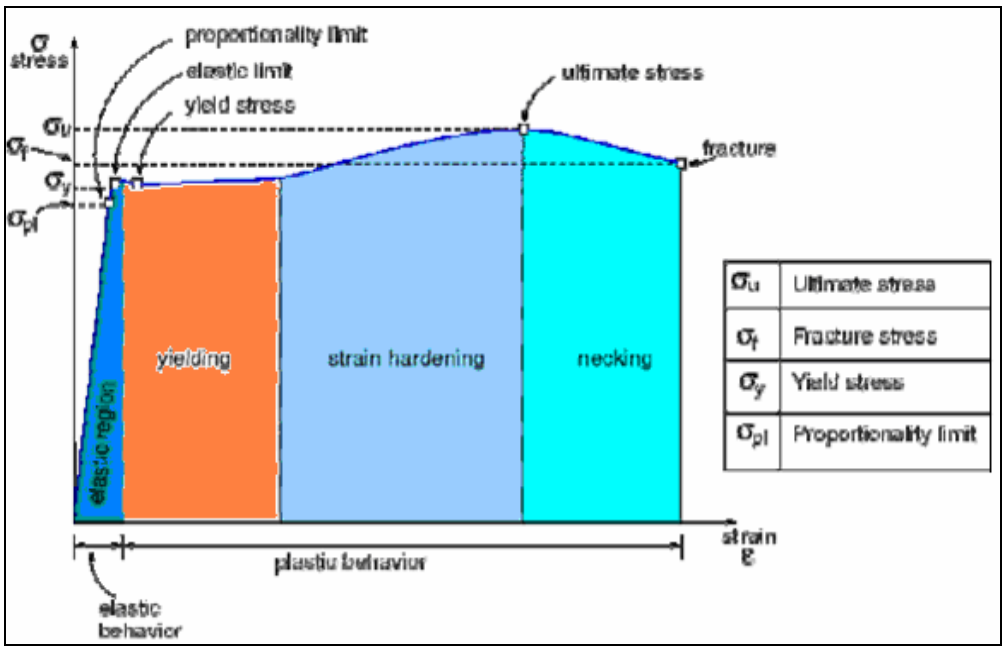

Fig. 1.3: Various regions and points on the stress-strain curve

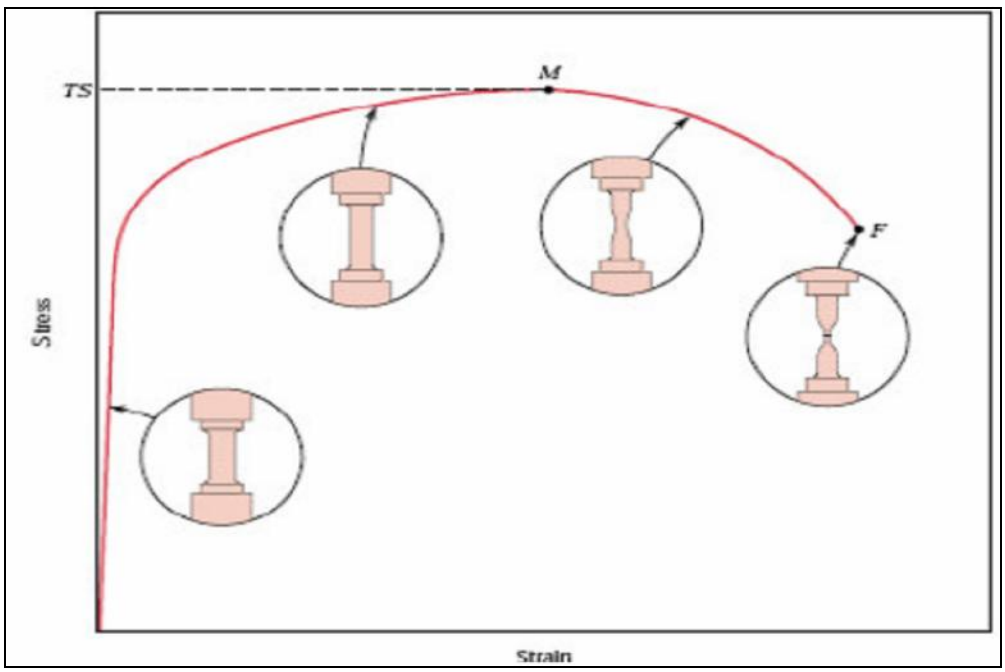

Fig. 1.4: Typical engineering stress–strain behaviour to fracture, point F

The tensile strength TS is indicated at point M. In Fig. 1.4 the circular insets represent the geometry of the deformed specimen at various points along the curve.

Engineering stress and strain measures incorporate fixed reference quantities. This is for undeformed cross-sectional area. True stress and strain measures account for

changes in cross-sectional area by using the instantaneous values for area, giving more accurate measurements for events such as the tensile test.

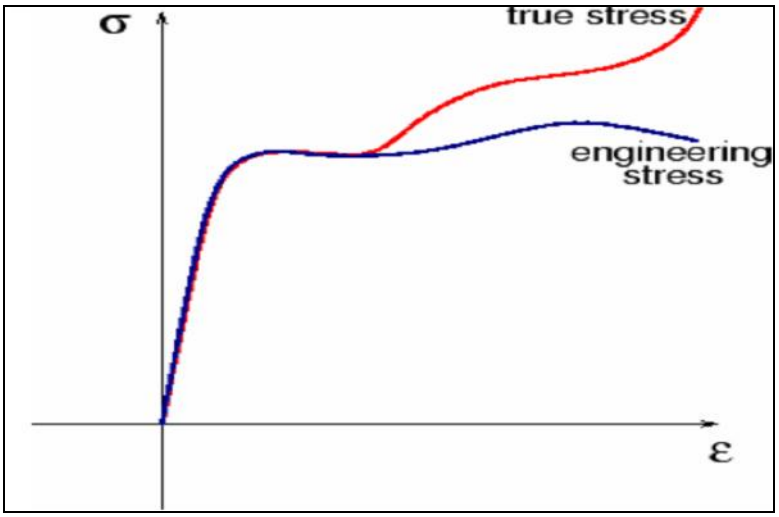

Fig. 1.5: Engineering stress-strain curve vs a true stress-strain curve

As the strain becomes large and the cross-sectional area of the specimen decreases, the true stress can be much larger than the engineering stress as shown in Fig. 1.5.

These tensile tests are to be conducted on Universal Testing Machine (UTM). UTM also known as a materials testing machine/ test frame which is used to test the tensile and compressive properties of materials. Such machines generally have two columns but single column types are also available. Load cells and extensometers measure the key parameters of force and deformation as the sample is tested. These machines are widely used and would be found in any materials testing laboratory.

The great benefit of the Universal Testing Machine is the dual testing capability, saving time for operators needing to change between fixtures, as they are fixed onto the machine at their own designated area. The operator needs only to switch a button on the machine to select from tensile to compression, which in turn speeds up production time, test set up time, reduces operator fatigue and decreases possible setup errors.

1.6 NON LINEAR ANALYSIS

There are three types of Nonlinearities which can be encountered during nonlinear analysis of any problem.

1. Geometric Nonlinearity.
2. Material Nonlinearity.
3. Changing initial/boundary conditions.

The geometric Nonlinearity arises purely from geometric consideration (e.g. nonlinear strain-displacement relations). The material nonlinearity is due to nonlinear constitutive behaviour of the material of the system .The third type of nonlinearity may arise due to changing initial or boundary conditions.

Nonlinear analysis is a necessity in

a) Designing high performance and efficient components of certain industries (e.g. aerospace, defense and nuclear).
b) Assessing functionality (e.g. residual strength and stiffness of structural elements) of existing systems that exhibit some types of damage and failure.
c) Establishing causes of system failure.
d) Simulating true material behaviour of the process.
e) Research to gain a realistic understanding of physical phenomena.

1.7 PRESENT DESIGN CONSIDERATIONS

Tension members used in building construction are designed according to the American Institute of Steel Construction building specifications LRFD [4] and ASD [3]. LRFD [4] requires that the designer make calculation checks to determine the capacity of a tension member: yielding of the gross cross-sectional area**;** net section rupture of the critical cross-sectional area**;** block shear**;** bolt bearing and bolt shearing. The lower of these controls the allowable load capacity of a specified member.

1.7.1 Gross Section Yielding

Yielding of the cross-section at service loads is considered to be a serviceability criterion so as to prevent large elongations of a member. Yielding of the net section area is not considered because the length, over which its gross area is reduced, due to connection details, is small compared to the overall length of the member. Therefore, significantly larger elongations than yielding of the gross area would not occur. Gross section yielding is calculated in LRFD [4] as follows:

$$P_n = F_y A_g \tag{1.2}$$

where F_y represents the yield stress of the material and A_g represents the gross cross sectional area of the tension member. Fig. 1.6 shows gross cross-sectional area.

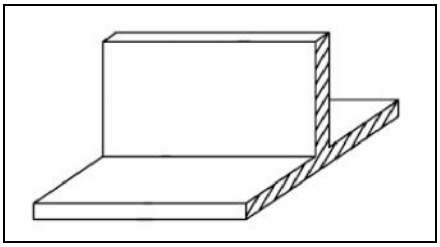

Fig. 1.6: Gross cross-sectional area

1.7.2 Net Section Rupture

The net section rupture strength of a member is based on the fracture of the net area of the cross-section. The net section rupture equation is given by.

$$P_n = F_u A_e \tag{1.3 a}$$

where

$$A_e = UA_n, \tag{1.3 b}$$

where F_u is the ultimate tensile strength of the material, A_n the net area of the cross-section, and A_e the effective net area of the cross-sections. Fig. 1.7 shows net cross-sectional area.

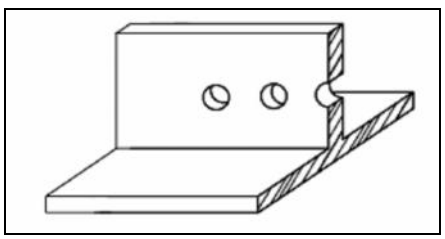

Fig. 1.7: Net cross-sectional area

In the eq. (1.3 b), *U* represents the shear lag reduction factor that accounts for member's inefficiency due to the inability of its elements to transfer load in a connected region. The reduction effects due to shear lag need be considered when only some of the elements of a member transfer load. The calculation of the shear lag factor according to LRFD [4] is given as

$U = 1.0$ for a member with all of its elements transferring load (1.4)

Else

$$U = 1-(x/L) < 0.9 \quad (1.5)$$

In eq. (1.5), x represents the connection eccentricity and L represents the connection length. From the above equation, it is clear that the effects of connection eccentricity and connection length have been combined into one factor in estimating the failure capacities of tension members. This equation is based on the test data with small connection eccentricities. Using the above equation for medium to large connection eccentricities often results in a small or negative U factor. Furthermore, recent efforts on investigating the effect of shear lag on failure capacities demonstrated that AISC predicted failure capacities using the above equation may be overly unconservative for large connection eccentricities. This forms the motivation for the current study to investigate the effect of connection eccentricity and connection length on the failure capacities of tension members with bolted end connections.

1.7.3 Block Shear

The most accurate model for block shear failures seemed to be the rupturing of the net tension plane and yielding on the gross shear plane, which increases towards a rupturing of the shear plane as connection lengths become shorter. This study led to the development of the present LRFD equations. The LRFD block shear provisions incorporate two possible modes of failure: rupture of the net tension area combined with simultaneous yielding of the gross shear area; or yielding of the gross tension area combined with simultaneous rupture of the net shear area. Fig. 1.8 shows these two types of block shear failure modes. The two LRFD block shear equations are shown below:

$$R_n = F_u A_{nt} + 0.6F_y A_{gv} \quad (1.6)$$

$$R_n = F_y A_{gt} + 0.6F_u A_{nv} \quad (1.7)$$

The controlling equation being the one with larger net area rupture term *i.e.* if $F_u A_{nt} \geq 0.6F_u A_{nv}$ then eq. (1.6) is used, else the eq. (1.7) is used to calculate the allowable block shear capacity. It is interesting to note that in design typically the eq. (1.7) governs, while experiments in which block shear is evident tend to exhibit a

failure mode similar to that described by eq. (1.6). Fig.1.9 shows the failure of typical design. This ambiguity in code prediction equations and experimental results forms the motivation for the current study to investigate the block shear failure of WT specimens.

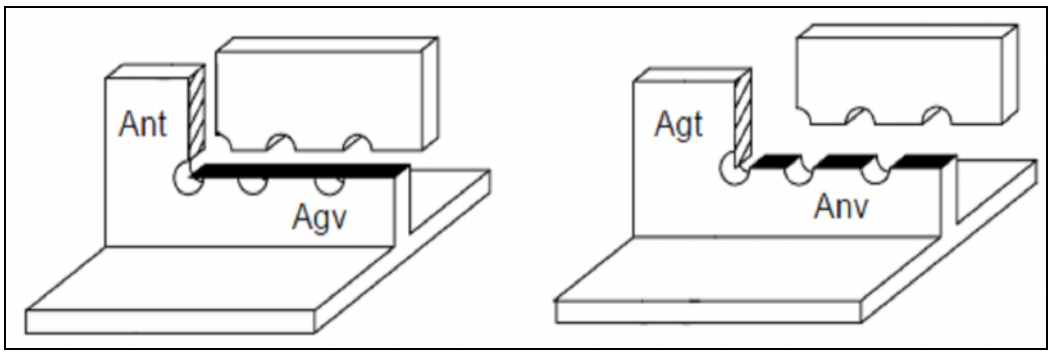

Fig. 1.8: Block shear

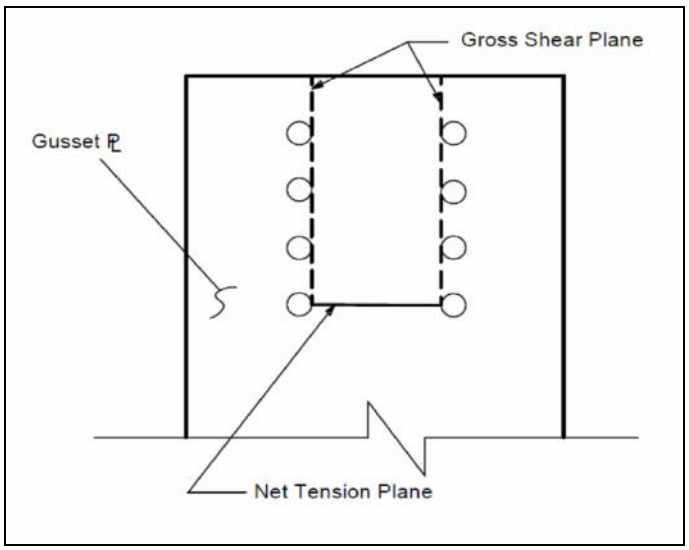

Fig. 1.9: Typical gusset plate failure

1.7.4 Bolt Bearing

Bolts are considered to transfer force between the connected members in one of two ways. One of the ways bolts transfer force is by what we call "bearing".

The bearing method assumes that the bolt contacts the side of a hole and there is a compressive force between the bolt and the side of the hole. The magnitude of this compressive force is limited by the strength of the member's material to handle this compressive force. And the bearing stress acts on the outside of the bolt and the inside

walls of the hole. Due to this, the bolt hole becomes of an oval shape and hence the joint becomes loose. The failure in such a manner is also known as *crushing failure*.

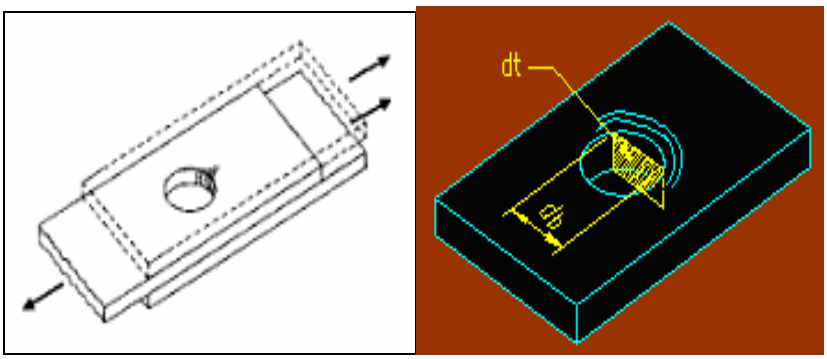

Fig. 1.10: Bearing failure

If the connected plates are made of high strength steel then failure of bolt can take place by bearing of the plates on the bolts. If the plate material is weaker than the bolt material, then failure will occur by bearing of the bolt on the plate and the hole will elongate. The bearing deformation limit state is based on a maximum bearing stress times the projected area of the contact surface normal to the direction of force. The area is shown in Fig. 1.10 and equals the actual diameter of the bolt times the thickness of the plate.

∴ Total bearing area,

$$A_b = d_b \times t \tag{1.8}$$

And bearing strength of a bolt is given by,

$$R_n = 3.0 n d_b . t . F_u n \tag{1.9}$$

where R_n is the bearing capacity, F_u is the ultimate tensile strength for the material, n is the number of bolts per pitch length, d_b is the diameter of bolt and t is the thickness of the plate.

1.7.5 Bolt Shearing

The plates which are connected by the bolts exert tensile stress on the bolts, and if the bolts are unable to resist the stress, they are sheared off as shown in

Fig.1.11.The resistance offered by a rivet to be sheared off is known as shearing strength or shearing resistance.

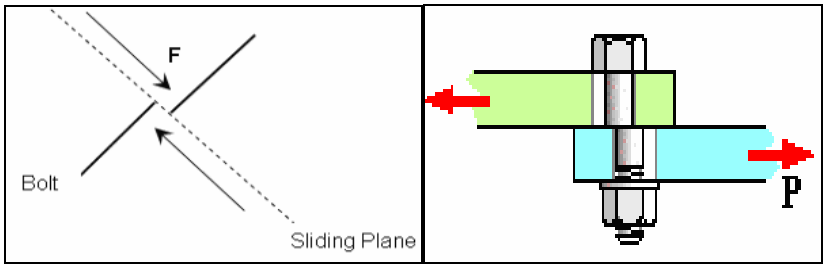

Fig. 1.11: Shearing of bolts

It may be noted that when the tangential force is resisted by one cross-section of the bolt then the bolts are said to be in single shear as shown in Fig. 1.12 (a). And if the tangential force is resisted by two cross-sections of the bolt then the bolts are said to be in double shear as shown in Fig. 1.12 (b).

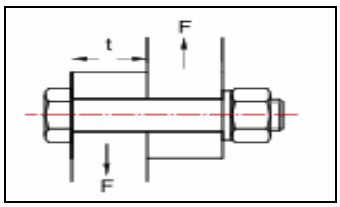

Fig. 1.12: (a) Bolt in single shear

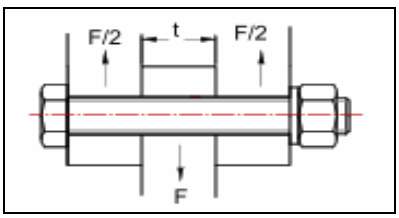

Fig. 1.12: (b) Bolt in double shear

Shearing strength or shearing resistance required to shear off the bolt per pitch length is given by:

$$R_n = n \times \frac{\pi}{4} \times d_b{}^2 \times \tau \qquad \text{(In single shear)} \qquad (1.10)$$

$$R_n = n \times 2 \times \frac{\pi}{4} \times d_b{}^2 \times \tau \qquad \text{(In double shear)} \qquad (1.11)$$

where R_n is the shearing capacity of bolt, τ is the shear stress for the bolt material, d_b is the diameter of bolt and n is the number of bolts per pitch length.

1.8 FINITE ELEMENT METHOD

In Finite Element Method, a complex region of defining a continuum is discretized into simple geometric shapes called 'Elements'. The material properties

and the governing relationships are considered over these elements in term of unknown values at element corner. An assembly process, duly considering the loading and constraints, results in a set of equations which are solved for results.

The Finite Element Method has become a very powerful tool for the numerical solution of a wide range of application. The application ranges from deformation & stress analysis of automotive parts, aircraft, building & bridge structures etc. Finite element method not only give the behavioral insight of the different part of the structure but it also analyze the structure taking the individual behavior of these parts into consideration and because of this fact it is becoming popular with the engineering field. It is also the trend in industry that the results are acceptable only when solved using certain computer programs. The following section discusses elementary information about Finite Element Methods.

1.8.1 Brief History

Basic idea of the Finite Element Method originated from advances in aircraft structure analysis. Turner *et al.* [1] derived stiffness matrices for truss, beam and other elements and presented their findings in 1956. In the early 1960s, engineers used the method of approximate solution of problem in stress analysis, fluid flow, heat transfer and other areas. A book by Argyris in 1955 on energy theorems and matrix methods laid a foundation for further developments in Finite Element studies. The first look on Finite Element by Zienkiewicz and Chung was published in 1967. In the late 1960s and early 1970s, Finite Element Analysis was applied to non linear problems and large deformation. Oden's book on nonlinear continua in 1972. Mathematical foundations were laid in 1970s. Today, the developments in mainframe computers and availability of powerful microcomputer have brought this method within reach of students and engineers working in small industries.

1.8.2 Basic steps of Finite Element Method

Finite Element Method can be divided into several distinctive steps. Theoretical approach to the method and its different steps are as follow:

- **Discretization**

Discretization is the process of dividing domain of problem into small regions or sub domains known as elements. Corner points of elements are called nodes. Fig. 1.13 shows the most usual elements:

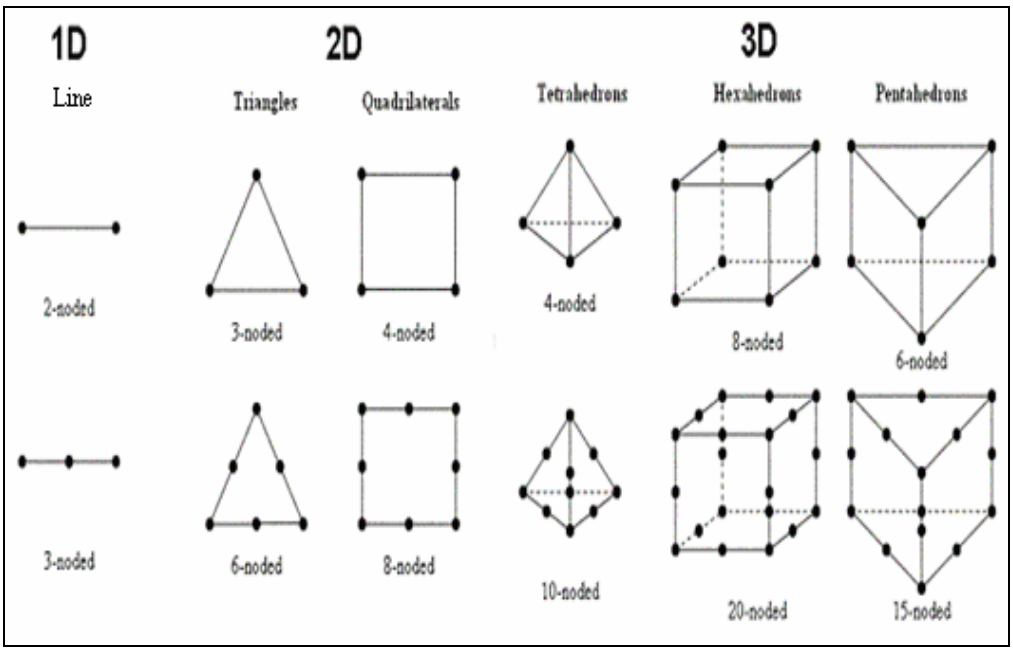

Fig. 1.13: Showing different types of elements

- **Element analysis / Element stiffness matrix**

The element analysis has two key components, expressing the variable within the elements, and maintaining equilibrium of the elements.

The governing equation is converted to algebraic form which is represented in matrix form and is called element equation or element stiffness matrix. This enables solution by computer. Element stiffness matrix represents the response of elements according to its property in the system for the parameters. Same matrix can be used for all elements of same type. Following steps are used for conversion of governing equation (differential or integral) into algebraic form-

- **Construction of trial solution**: - It is a cyclic process by hit trial. The equation with certain Degree of freedom (DOF) is taken, which is solved by applying boundary condition either at the starting for manual processing or after formulation of system stiffness matrix for solution through computer.

- **Application of optimization criteria**: - Optimization criteria are used to find the values of trial function. Various methods used for optimization are given below
  - Method of weighted residual
  - Collocation Method
  - Sub domain Method
  - Least square Method
  - Galerkin Method
  - Ritz Variational Method

- **Estimation of accuracy**: - The accuracy of solution is checked for closeness to exact solution. Also accuracy can be checked by checking the reducing difference of the consecutive solutions obtained by increasing degree of freedom known as Property of Convergence. Sources of error in FEM are
  - Domain Error: - Discretization of domain is approximate.
  - Computational Error: - Integration and differentiation induce error.
  - Approximation Error: - Assumption of D.O.F makes the solution approximate.

- **System analysis / system stiffness matrix**

The matrix equations for the individual elements are combined to form the Matrix equations for the entire system called system stiffness matrix. It gives the response of the parameters on the entire system.

- **Incorporation of boundary and loading conditions**

The system stiffness matrix is modified according to the over all boundary conditions. This reduces calculation work and saves time.

- **Solving of the system equations.**

The system equations can be solved to give the unknown values at the nodes. If the problem is of an equilibrium nature, then the solution is obtained by solving a set of linear or non-linear equations. System equations can be solved by number of available solvers like Gauss Elimination or Gauss Siedel etc.

- **Post processing / Display**

The post processing stage deals with the representation of results. Typically, the deformed configuration, mode shapes, temperature, and stress distribution are displayed at this stage.

Finite Element studies are useful when used in conjunction with an experimental testing program. Examining the block shear and net section rupture failure modes using a Finite Element Analysis (FEA) method allows for a more extensive parametric investigation of the underlying behavior than is possible in a laboratory setting**.** In previous years, much progress has been made in the Finite Element modeling of the net section rupture and block shear failure of tension members with bolted end connections. Finite element modeling of experimental specimens will allow for a better understanding of stress flow in the member and to better investigate the influence of shear lag and connection eccentricity.

CHAPTER 2
LITERATURE REVIEW

A lot of research work has been carried out throughout the world to investigate and analyze the behaviour of steel tension member subjected to uniaxial loading. A brief review of literature is being presented here.

2.1 LITERATURE REVIEW

Munse and Chesson [1] in 1963 studied riveted and bolted joints and examined factors that reduce net section capacity, conducted numerous experiments on various specimens and connection details. In addition to their own experiments they examined test results from extensive bolted and riveted tests. These tests included flat plates, single angles, double angles connected on the same side of the gusset plate, double angles connected on opposite sides of a gusset plate, built-up I-sections, single channel sections and double channel sections.

Prior to these studies, tension member capacity was based solely on gross section yielding or net section rupture. The net section rupture capacity calculations incorporated no allowance for net section efficiency or hole fabrication.

Based on the results of their studies and an investigation of the data from other studies, they were the first to propose an equation representing the “effective” net section. Their expression suggested that the net section effective area is a function of: material ductility, shear lag effects, net section area, and the ratio of the net to gross cross-sectional area.
This expression has the form:

$$A_e = A_n(1.60 - 0.7\frac{A_n}{A_g})(1-\frac{x}{L}) \qquad (2.1)$$

Ricles and Yura [2] in 1983 studied strength of double-row bolted-web connections and conducted full-scale testing of coped and uncoped double row bolted-web connections supplemented by an elastic FEA. The main objective of this analysis was to obtain elastic stress distributions in the vicinity of shear connector bolt

holes and to develop a modified block shear failure model which was in close agreement with the experimental results. The beam and the connection were assumed to be in a plane stress condition. The Finite Element model consisted of two dimensional four-node quadrilateral and three node triangular elements. The material response is modeled by an elastic stress–strain curve. The clip angle was idealized as a simple connection plate with attached springs to simulate the stiffness of the outstanding leg to the rotation of the clip angle. The results of the experimental and analytical studies showed that present block shear equations, which were the governing failure model for these experiments, did not accurately predict failure loads. They were developed a set of modified semi-empirical block shear expressions that captured the behaviour of the specimens in their study.

Gross *et al.* [5] in 1995 did block shear tests in high strength steel angles and Orbison *et al.* [8] in 1999 studied tension plane behaviour in single-row bolted connections subject to block shear. Both performed tests on WTs and single angles. Both stated that the failures observed were block shear; a yielding of the gross shear area and rupture of the net tension area. LRFD block shear predictions were on the average conservative for the WT tests. The specification prediction results produced were slightly un-conservative for the [5] angle tension tests. However, the specimen failures with large eccentricities from the present study did not show signs of extended yielding along the gross shear plane, but only local yielding of the shear plane in the vicinity of the lead bolt.

Epstein and Chamarajanagar [6] in 1996 discussed Finite Element studies for correlation with block shear tests and also discussed a parametric Finite Element study to capture the influence of bolt stagger spacing and shear lag effects on block shear failure of angles in tension. A 20-node brick element was used in the Finite Element modeling of the angle sections to capture the stress concentration effects in the vicinity of bolt holes. The material nonlinear effects were modeled using the von Mises yield criterion and the material stress–strain curve was assumed to be elastic–perfectly plastic. In the study, a strain based failure criterion in which failure was assumed to have occurred once the maximum strain reached five times the initial yield strain was employed to capture the failure load. Further, in the Finite Element Model, the bolts were assumed to be rigid and the load is transferred from the gusset

plate to the angle fully by the bearing of the bolts. Therefore, the longitudinal and the in-plane transverse displacements of the nodes attached to the bearing surfaces, i.e. the surfaces on which the bolt surface bears against a hole surfaces, were coupled to one another. This Finite Element study included only the material nonlinear effects and the geometric nonlinear effects were considered to be negligible. In all of the Finite Element simulations, failure was initiated at the outside edge of the connected leg adjacent to the lead bolt on the outer gage. From the experimental and finite element results, it was concluded that the shear lag effect present in these angles significantly reduced the load carrying capacity of the tension member.

Kulak and Wu [7] in 1997 studied shear lag in bolted angle tension members and examined shear lag effects and presented accountings for shear lag in American and Canadian design specifications (which are based on AISC LRFD specifications), conducted a number of tension tests of single and double angles with punch bolt holes, considering only net section rupture. The failure of these single and double angle specimens was preceded by a necking down of the net area between the leg edge and lead bolt hole. Rupturing of the specimen initiated at the leg edge and propagated through to the bolt hole and then on through the rest of the specimen.

Barth *et al.* [9] in 2002 studied behaviour of steel tension members subjected to uniaxial loading and performed load tests on three series of short tension member specimens to investigate the influence of varying connection eccentricity and connection length on the load capacity of the members. Additionally, studies were conducted to investigate the influence of hole fabrication methods. Two methods were used: punched holes and drilled holes. Rupture load capacity of the net section was observed to be significantly reduced with moderate connection eccentricity, and a net section efficiency factor was developed and proposed as a replacement for the current shear lag factor in determining the effective net area of a WT tension member.

Gupta and Gupta [10] in 2004 studied evaluation of stress distribution in bolted steel angles under tension and showed that the stress distribution in the vicinity of connections in a bolted steel angle is non-uniform because of the coupled effects of connection eccentricity, shear lag and stress concentrations. Although, some researchers have attempted finite element analysis, stipulations in various codes and

specifications regarding the design of angle tension members are primarily based on the experimental studies. Only a couple of previous studies had included geometric as well as material non-linear effects in such finite element analysis. They also presented the state-of-the-art review of finite element techniques used in modeling the angle tension members with bolted connections. That review was followed by a non-linear finite element analysis so as to obtain the stress distributions in the vicinity of connections, at design loads. They concluded that in three bolts and four bolts connections, the zones of high stresses lie primarily along the critical section in the connected and un-connected legs and in a two bolts connection, the stresses are mainly concentrated on the connected leg only, and in the un-connected leg, the stresses are relatively low.

Pan [11] in 2004 studied the prediction of the strength of bolted cold-formed channel sections in tension and investigated the shear lag effect in bolted cold formed steel tension members. Channel sections with different dimensions tested by using bolted connections were discussed in this study. The comparisons were made between the test results and predictions computed based on several specifications. In order to study the stress distribution at the various locations of the cross-section of specimen, the Finite-Element software ANSYS was also utilized in this research. Shear lag effect occurs when some elements of the tension member are not connected. This effect reduces the strength of the member because the stresses distributed over the entire section are not uniform. The average value of stresses on the net section may thus be less than the tensile strength of the steel. The reduced strength of the member can be expressed as the efficiency of the net section. Based on these experiments, a mathematical model was developed and a new expression for the reduction coefficient “U” was suggested.

The expression had the form

$$U = [1.15 - 0.86\left(\frac{\bar{x}}{L}\right) - 0.14\left(\frac{W_u}{W_c}\right) \qquad (2.2)$$

where $\bar{x}$ is the connection eccentricity , L is the connection length , Wu is the length of unconnected elements, and Wc is the length of connected elements, shown in Fig.2.1.

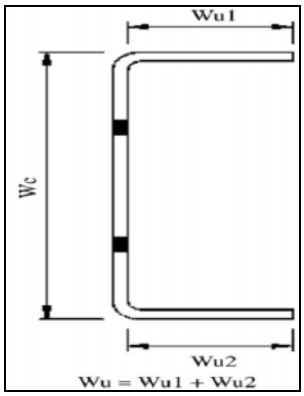

Fig. 2.1: Definitions of Wu and Wc

Topkaya [12] in 2004 discussed finite element parametric studies on block shear failure of steel tension members and conducted tests to develop simple block shear load capacity prediction equations that are based on Finite Element Analysis. Over a thousand nonlinear analyses were performed to identify the important parameters that influence block shear capacity. In addition, the effects of eccentric loading were investigated. Based on the parametric study block shear load capacity prediction equations were developed. The predictions of the developed equations were compared with the experimental findings and were found to provide estimates with acceptable accuracy. The predicted equation was:

$$R_n = 0.48F_u A_{gv} + F_u A_{nt} \tag{2.3}$$

Michael *et al.* [13] in 2007 discussed the block shear strength of coped beams with a welded clip angle connection experimentally. The ends of a coped beam are commonly connected to the web of a girder by double clip angles. One of the potential modes for the failure of the clip angle connection is the block shear of the beam web material. The test parameters included the aspect ratio of the clip angles, the web shear and tension area around the clip angles, the web thickness, beam section depth, cope length, and connection position. The test results indicated that the specimens failed, developing either tension fractures of the web near the bottom of the clip angles or local web buckling near the end of the cope. Although the final failure mode of the six specimens was local web buckling, it was observed during the tests that these specimens exhibited a significant deformation of the block shear type prior to reaching their final failure mode. No shear fracture was observed in all of the tests.

Michael *et al.* [14] in 2007 discussed the block shear strength of coped beams with a welded clip angle connection numerically and conducted experiment to gain a better understanding of the connection behaviour, such as the stress distribution in the web near the periphery of the clip angles and the failure mechanism of the connection, an analytical study of the block shear capacity of coped beams with welded clip angles was carried out using the finite element method. Based on the limited test data and the results of the Finite Element Analysis, a strength model was established and a design equation was proposed to evaluate the block shear strength of coped beams with welded clip angles. It was shown that the proposed design equation gave better predictions of the block shear capacity of the specimens.

Paula *et al.* [15] in 2008 studied efficiency reduction due to shear lag on bolted cold-formed steel angles and fined the capacity of cold-formed steel members under tension and connected with bolts. This research was particularly interested in the shear lag phenomenon which influences the net-section capacity by means of a reduction coefficient. This reduction was computed through the reduction coefficient which is a function of two parameters: length of the connection and distance of the shear plane to the centroid of the cross-section. Sixty-six experimental tests carried out on cold-formed steel angles fastened with bolts and under tension in the laboratory and the results are reported here together with other experiments reported in the literature. Based on these experiments, a mathematical model was developed and a new expression for the reduction coefficient "U" was suggested.
The expression had the form

$$U = 1.19 - 0.26\frac{\bar{x}}{L} - (0.63b_{cn} + 0.17b_d - 0.47d - 1.70t)/b_c \qquad (2.4)$$

where $\bar{x}$ is the connection eccentricity, L is the connection length L, b_c is the width of the angle connected leg, b_{cn} is the net width of the angle connected leg, b_d is the width of the unconnected leg, d is the nominal bolt diameter, and t is the angle thickness, shown in Fig. 2.2.

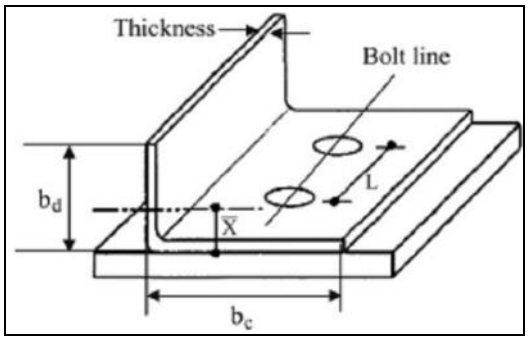

Fig. 2.2: Cold-formed angle for a bolted connection

Bouchair *et al*. [16] in 2008 studied analysis of the behaviour of stainless steel bolted connections and conducted experiments on two types of bolted connections that were common in steel structures. They concerned cover plate connections and T-stubs, where the bolts were loaded in shear or in tension. The requirements for stainless steel connection design were essentially the same as for carbon steel. The study considered the case of austenitic stainless steel for which the conventional elastic limit was relatively low compared to the ultimate strength. In bearing, criteria on deformation limits have to be considered for cover plate connections. In T-stubs, strain hardening of stainless steel exhibits a continuous increase of the applied load and can influence the failure mode. A Finite Element Model is developed and validated for the two types of connections. A more extensive parametric study should be carried out to develop a better understanding of the behaviour of stainless steel connections.

Ranawaka and Mahendran [17] in 2008 discussed experimental study of the mechanical properties of light gauge cold-formed steels at elevated temperatures. In recent times, light gauge cold-formed steel sections have been used extensively as primary load bearing structural members in many applications in the building industry. Fire safety design of structures using such sections has, therefore, become more important. Deterioration of mechanical properties of yield stress and elasticity modulus is considered the most important factor affecting the performance of steel structures in fires. A research project based on experimental studies was, therefore, undertaken to investigate the deterioration of mechanical properties of light gauge cold-formed steels. Tensile coupon tests were undertaken to determine the mechanical properties of these steels made of both low- and high-strength steels and thicknesses

of 0.60, 0.80 and 0.95mm at temperatures ranging from 20 to 800^{o} C. Test results showed that the currently available reduction factors are unsafe to use in the fire safety design of cold-formed steel structures. Therefore, new predictive equations were developed for the mechanical properties of yield strength and elasticity modulus at elevated temperatures. The work presented the details of the experimental study and the results, including the developed equations. It also included details of a stress–strain model for light gauge cold-formed steels at elevated temperatures.

Chakherlou *et. al.* [18] in 2008 studied the experimental and numerical investigation of the effect of clamping force on the fatigue behaviour of bolted plates. In the experimental part of the research, a holed plate was clamped using a bolt and a nut, and then tested under axial cyclic load in a fatigue testing machine. In order to obtain S–N curves and investigate the direct effect of the isolated clamping force on the fatigue behaviour of the bolted plates, three batches of specimens each subjected to different clamping forces were fatigue tested. The clamping forces were obtained experimentally from the compressive axial strain of a steel bush which was placed between the nut and the plate. In the numerical method, to determine the stress and strain distributions due to combined clamping force and axial load in plate, 3D finite element models were generated using a numerical package. Numerical simulation and experimental results showed that the fatigue life of bolted plates improve because of the compressive stresses created around the plate hole due to clamping force. The life improvement was greatest at the high cycle fatigue life region of the S–N curves.

The above study reveals that a lot of work is done in the field of failure of tension members, strength of bolted joints, shear lag effect in bolted tension members and effect of connection eccentricity and connection length on the failure capacities of tension members with bolted end connections. But a study was not developed in which the connection length is increased by changing the pitch not by increasing the number of bolts. Thus the effect of increasing connection length by increasing pitch along with connection eccentricity is aimed to be done in present work. Thereafter the Finite Element Analysis is also used to compare these results.

CHAPTER 3
EXPERIMENTAL SET UP

3.1 GENERAL

The tension test is used to ascertain several mechanical properties of materials that are important in design. The results of tensile tests are used in selecting materials for engineering applications. Tensile properties are often measured during development of new materials and processes, so that different materials and processes can be compared. Finally, tensile properties are often used to predict the behavior of a material under different forms of loading.

The strength of interest may be measured in terms of either the stress necessary to cause appreciable plastic deformation or the maximum stress that the material can withstand. These measures of strength are used, with appropriate caution (in the form of safety factors), in engineering design.

The purpose of the present work is to investigate the effect of connection eccentricity and connection length on the failure capacities of WT tension members with bolted end connections. In this the connection length is increased by changing the pitch not by increasing the number of bolts.

Besides the strength of the member, strain distributions at the critical section corresponding to stress and the deformations of the specimens corresponding to load were also examined. A total of six specimens were tested. Only one line of bolts was considered. All tests were performed at Thapar University using 1000 kN Universal Testing Machine.

3.2 SPECIMENS GEOMETRIES

The experimental testing consists of two sets of short WT tension specimens fabricated from rolled steel. All specimens are of 600 mm length. All specimens are fastened, with a single row of 15 mm A490 bolts, through their webs at both ends, shown in Fig. 3.1 and Table 3.1. The tests consist of the 2 sets of WT 90x2 specimen

with the same eccentricities, but different connection lengths *i.e.* 50 mm and 75 mm. Connection length was increased or decreased by varying the pitch. The end distance and number of bolts for each specimen are held constant at 42 mm and 3 respectively. Holes for the 15 mm A490 bolts were specified to be drilled to a 16 mm diameter.

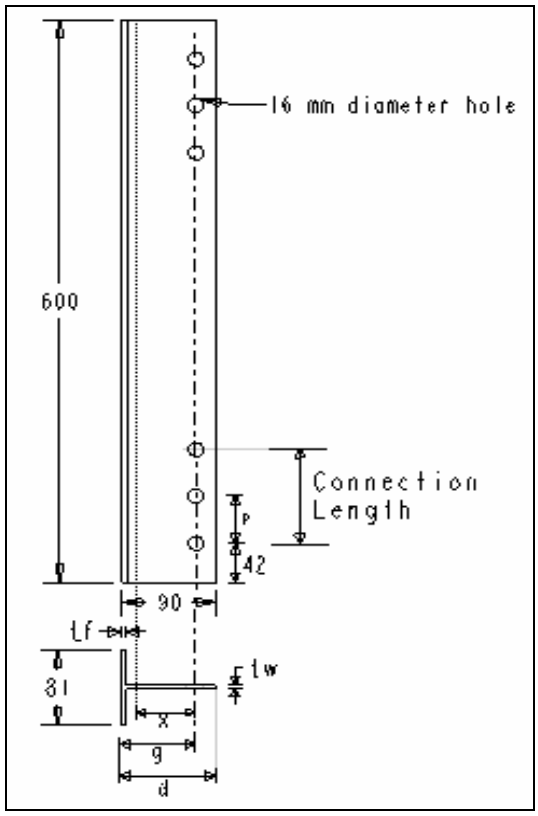

Fig. 3.1: Typical WT specimen configuration

Table 3.1: Specimen Dimensions and Material Strengths (All dimensions in mm)

Spec. No.	No. of Bolts	End Distance	Conn. Length L	Gage Distance g	Bolt Line Eccentricity x	Spec. Depth d	Web Thickness tw	Flange thickness tf	Hole Dia. dh	Yield Strength (MPa)	Tensile strength (MPa)
WT1	3	42	100	70	48.6	90	4	6	16	250	460
WT2	3	42	100	58	36.6	90	4	6	16	250	460
WT3	3	42	100	46	24.6	90	4	6	16	250	460
WT4	3	42	150	70	48.6	90	4	6	16	250	460
WT5	3	42	150	58	36.6	90	4	6	16	250	460
WT6	3	42	150	46	24.6	90	4	6	16	250	460

The present study has particular focus placed upon the effects of connection eccentricities with regards to induced bending moments. The specimens' eccentricities were specified such that a broad range of eccentricities could be examined. As past results have shown, connection length has significant influence on

the failure capacity. So in present study connection length was varied by increasing and decreasing the pitch. The specification requires that a pitch no less than 2.75*d* (where "*d*" is the nominal bolt hole diameter) is to be used in design and that a pitch distance of 3d is more appropriate for connections. Typically, 50 mm and 75 mm pitches are used in construction practices for 16 mm diameter bolts. These specimen geometries are shown in Fig. 3.2.

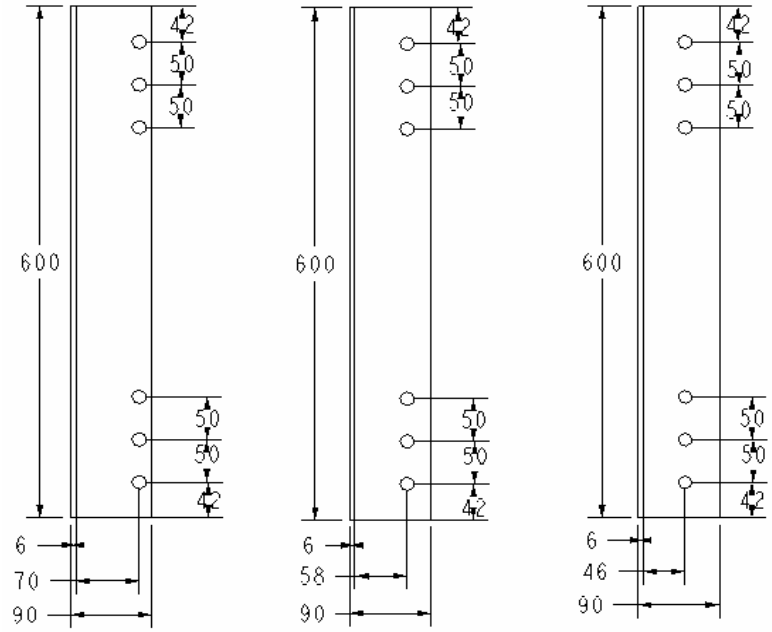

(a) WT 1 **(b) WT 2** **(c) WT 3**

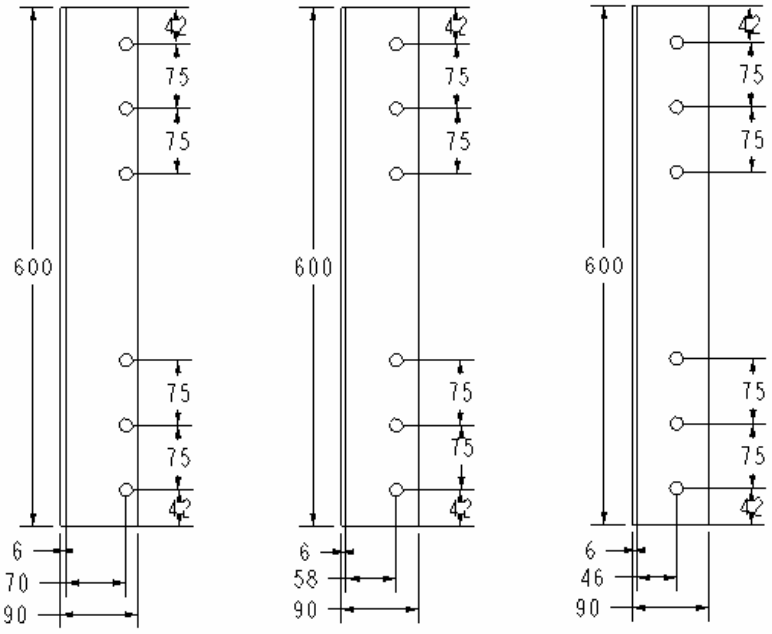

(d) WT 4 **(e) WT 5** **(f) WT 6**

Fig. 3.2: WT 90x2, 3 bolt connection specimen geometry (Rolled steel, 4 mm thick web, bolt holes are 16 mm in diameter)

3.3 EXPERIMENTAL TEST SET-UP

The experimental tests were carried out using Universal Testing Machine shown in Fig 3.3. After the appropriate grips were fastened to a WT the specimen-grip assembly was then placed and centered in the UTM and then secured fast grips in the UTM grippers shown in Fig. 3.4. Each specimen was tested to failure by steadily increasing the applied load. With all instrumentation zeroed, the tensile load was then applied in control with strain rate of 1.8 mm per minute. Stress-Strain and static load-deformation readings were obtained. Sigma plot was used to monitor the stress versus strain and load versus elongation behavior of the test.

Fig. 3.3: Universal Testing Machine HT-2101A (HUNGTA) Universal

Fig. 3.4: Specimen grip assembly in UTM

Bar stock grips, are used to transfer the load from a HUNGTA 1000 KN universal testing machine (UTM) to a WT specimen. They are fabricated from 62.5 mm by 16 mm mild steel bar stock and had 16 mm diameter holes drilled at the appropriate pitch. Two sets of bar stock grips were used in this study. One set of grips had 50 mm pitch holes, while the other set had 75mm pitch holes drilled on each bar. The 50 mm pitch holes bar stock grips have a length of 300 mm and the 75 mm pitch holes bar stock grips have a length of 350 mm. Fig. 3.5 shows the sketches with appropriate dimensions of the two types of grip used.

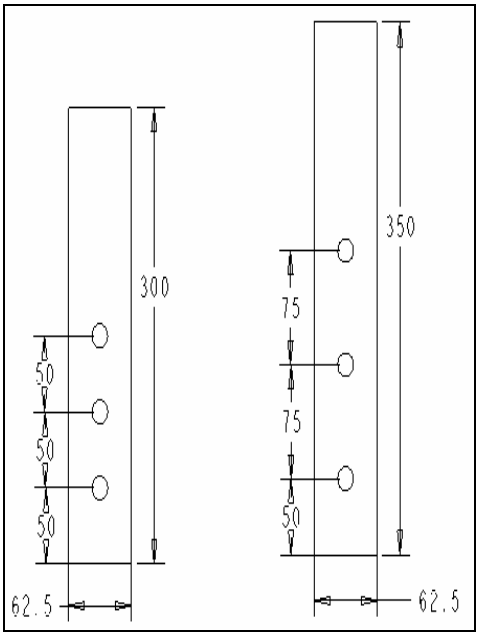

Fig. 3.5: Bar stock grip geometry having 50 mm pitch & 75 mm pitch (Mild steel, 16 mm thick and bolt holes are 16mm in diameter)

To prevent bending of the grip ends and, thus, enabling the UTM wedge-grips to have a truer contact surface with the bar stock grips, spacer plates of the same thickness as a specimen's web were placed between the ends of the grips. Fig. 3.6 shows a typical WT specimen with attached grips, a specimen-grip assembly. The bolts were tightened to the snug-tight condition, which allowed the specimens to go into bearing after the initial loading of a specimen. Bolts were reused for tests if they were visually undamaged from previous tests.

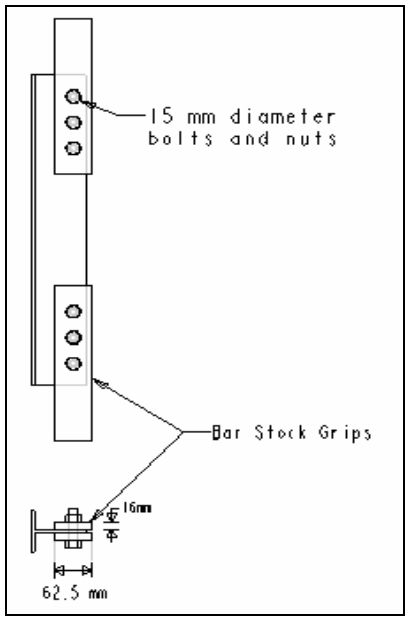

Fig. 3.6: Typical WT specimen-grip assembly

3.4 EXPERIMENTAL RESULTS

The experiments were carried out on six WT specimens, WT 1, WT 2, WT 3, WT4, WT5 and WT 6 as shown in Fig. 3.2. The results of above experiments are detailed below:

- **SPECIMEN WT 1**:

Table 3.2: Experiment results for specimen WT 1

EXPERIMENT WT 1			
FORCE (kN)	DISPLACEMENT (mm)	STRESS (MPa)	STRAIN
0.00	0.00	0	0.0000
5.00	1.20	5	0.0013
10.00	3.14	10	0.0024
15.00	4.00	15	0.0029
20.00	4.80	20	0.0044
25.00	5.30	25	0.0056
30.00	5.80	30	0.0068
35.00	6.30	35	0.0079
40.00	6.60	40	0.0086
45.00	7.00	50	0.0101
50.00	7.40	60	0.0114
55.00	7.85	70	0.0126
60.00	8.20	80	0.0139
65.00	8.50	90	0.0149
70.00	9.15	100	0.0166
75.00	9.55	110	0.0182
80.00	10.20	115	0.0192
85.00	10.75	120	0.0203
90.00	11.25	125	0.0213
95.00	12.10	130	0.0225
100.00	12.73	135	0.0237
105.00	13.70	140	0.0254
110.00	14.80	143	0.0262
113.00	15.35	140	0.0268
115.00	15.87	135	0.0273
117.20	16.53	130	0.0276
115.00	16.70	125	0.0279

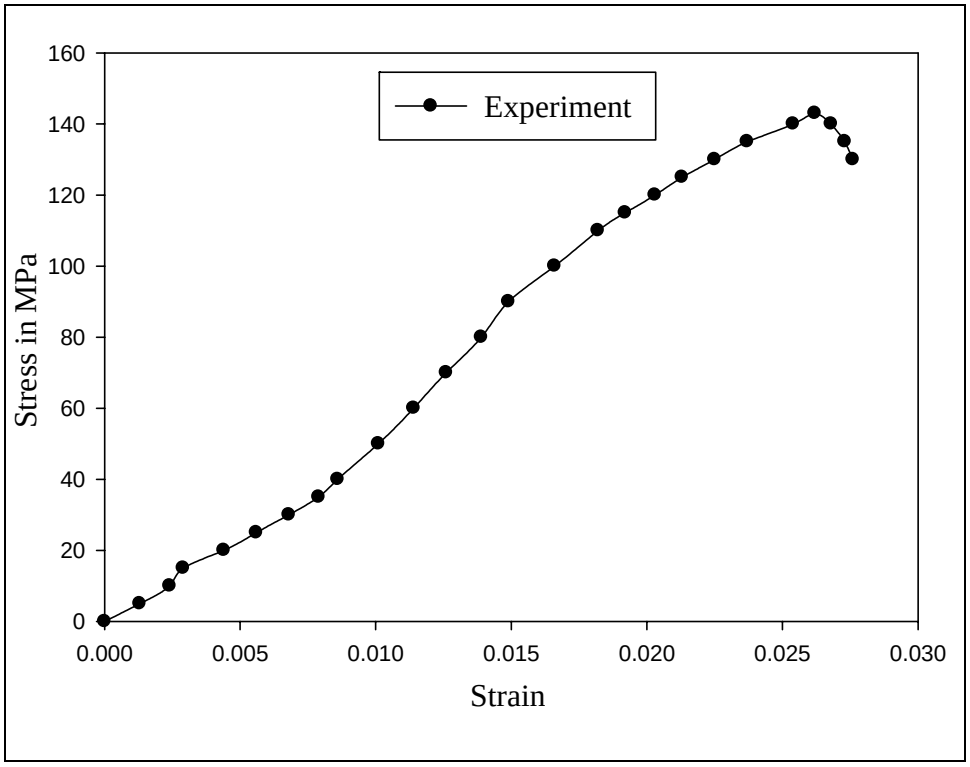

Fig. 3.7: Graph between stress and strain for specimen WT 1

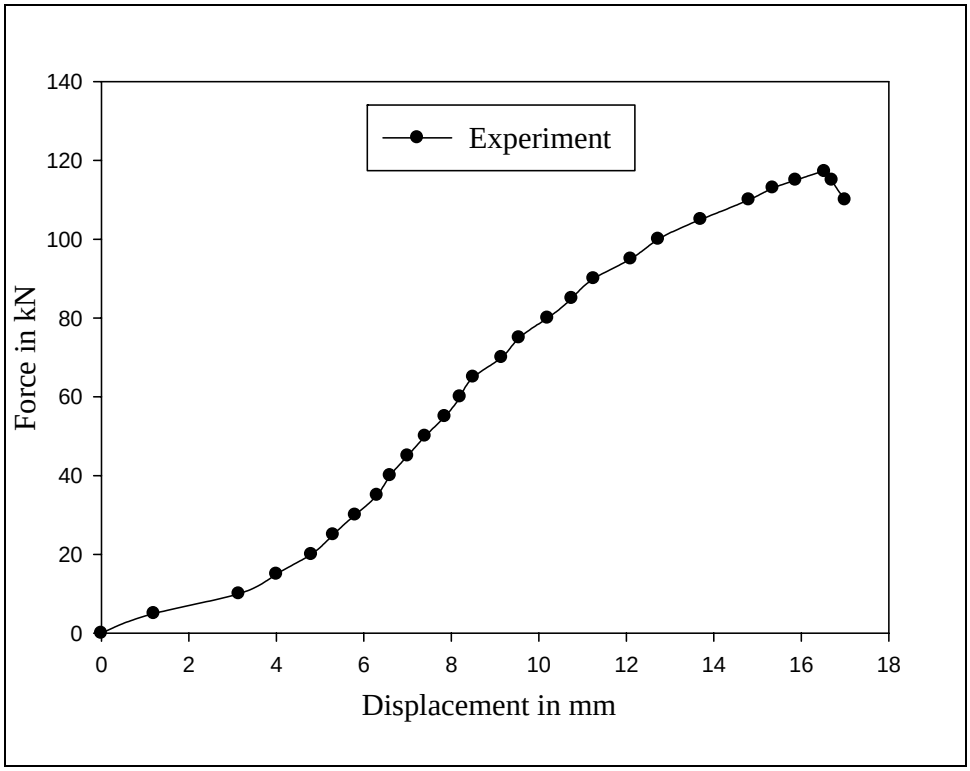

Fig. 3.8: Graph between force and displacement for specimen WT 1

- **SPECIMEN WT 2**:

Table 3.3: Experiment results for specimen WT 2

EXPERIMENT WT 2			
FORCE (kN)	DISPLACEMENT (mm)	STRESS (MPa)	STRAIN
0.00	0.00	0	0.0000
5.00	1.10	5	0.0015
10.00	2.05	10	0.0029
15.00	2.70	15	0.0040
20.00	3.15	20	0.0054
25.00	3.70	25	0.0065
30.00	4.10	30	0.0076
35.00	4.51	35	0.0086
40.00	4.92	40	0.0.92
45.00	5.60	50	0.0106
50.00	6.20	60	0.0117
55.00	6.95	70	0.0129
60.00	7.60	80	0.0136
65.00	8.12	90	0.0146
70.00	8.70	100	0.0156
75.00	9.25	110	0.0165
80.00	10.00	120	0.0174
85.00	10.45	130	0.0184
90.00	10.88	140	0.0197
100.00	11.65	145	0.0207
110.00	12.62	150	0.0216
120.00	13.50	155	0.0230
130.00	14.25	160	0.0244
140.00	15.45	165	0.0260
150.00	16.70	170	0.0271
152.00	17.15	174	0.0292
150.00	18.05	170	0.0313
145.00	18.50	165	0.0320

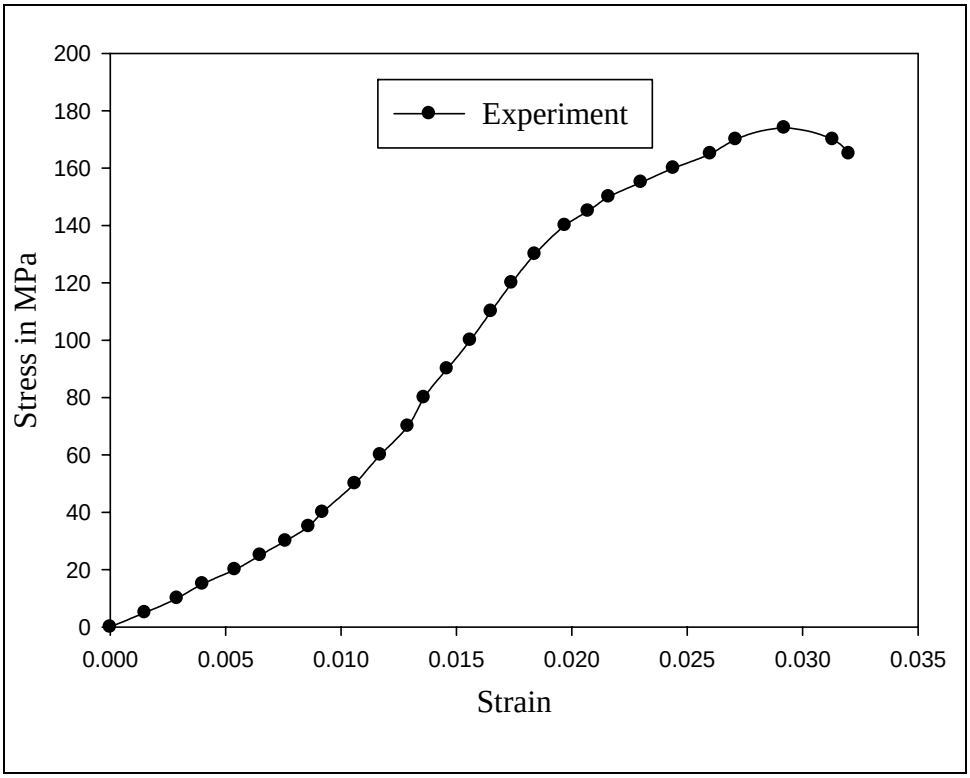

Fig. 3.9: Graph between stress and strain for specimen WT 2

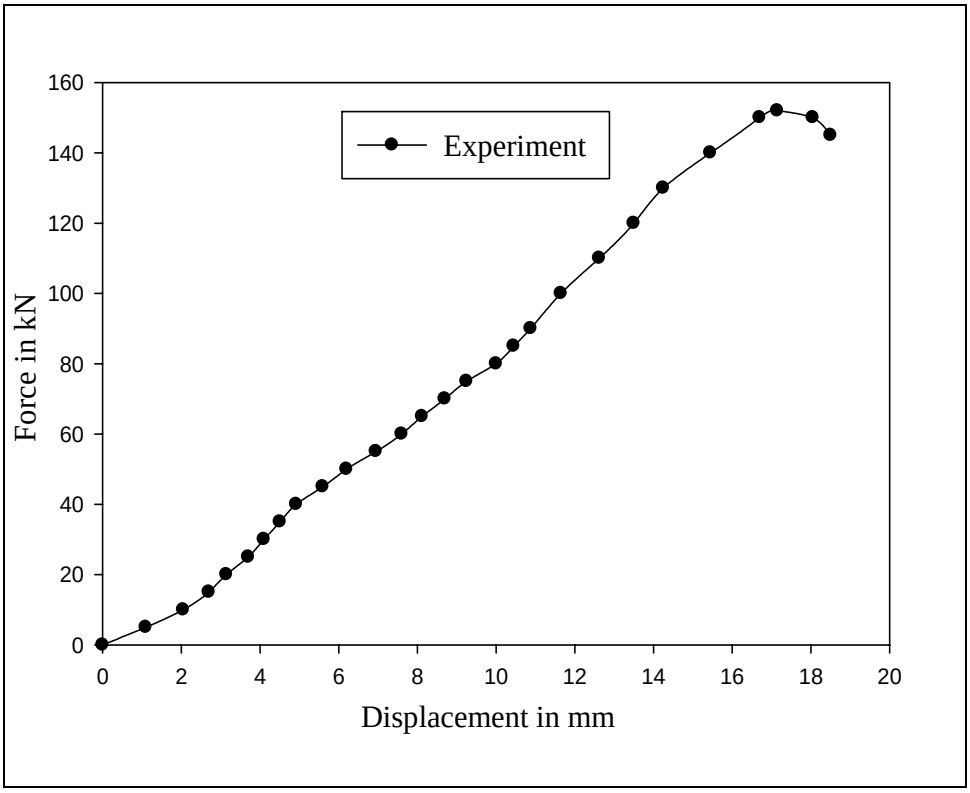

Fig. 3.10: Graph between force and displacement for specimen WT 2

- **SPECIMEN WT 3**:

Table 3.4: Experiment results for specimen WT 3

EXPERIMENT WT 3			
FORCE (kN)	DISPLACEMENT (mm)	STRESS (MPa)	STRAIN
0.00	0.00	0	0.0000
5.00	2.42	5	0.0032
10.00	4.24	10	0.0056
15.00	4.95	20	0.0080
20.00	5.40	30	0.0091
25.00	5.90	40	0.0103
30.00	6.42	50	0.0112
35.00	6.87	60	0.0121
40.00	7.35	70	0.0131
50.00	8.20	80	0.0140
60.00	8.80	90	0.0150
70.00	9.32	100	0.0160
80.00	9.90	110	0.0167
90.00	10.40	120	0.0173
100.00	10.88	130	0.0180
110.00	11.40	140	0.0187
120.00	12.10	150	0.0195
130.00	12.86	160	0.0210
140.00	13.70	170	0.0218
150.00	14.55	180	0.0232
160.00	15.50	190	0.0244
165.00	16.18	200	0.0260
170.00	17.00	205	0.0269
172.00	17.30	210	0.0280
174.00	17.86	215	0.0300
176.00	18.28	216	0.0309
177.50	19.10	210	0.0325

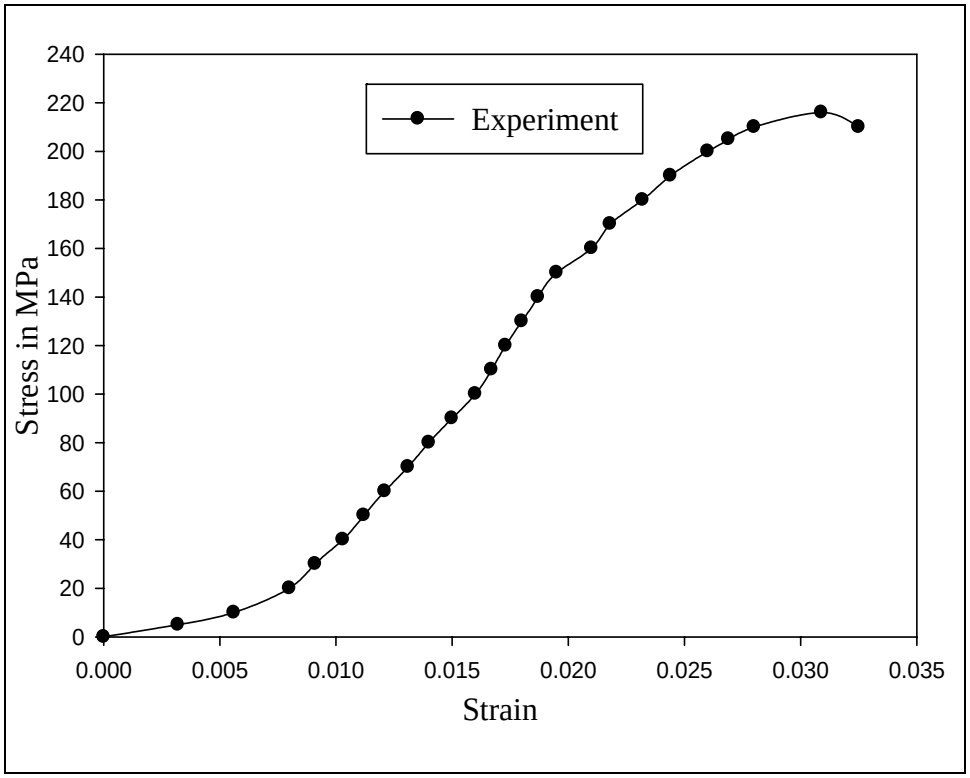

Fig. 3.11: Graph between stress and strain for specimen WT 3

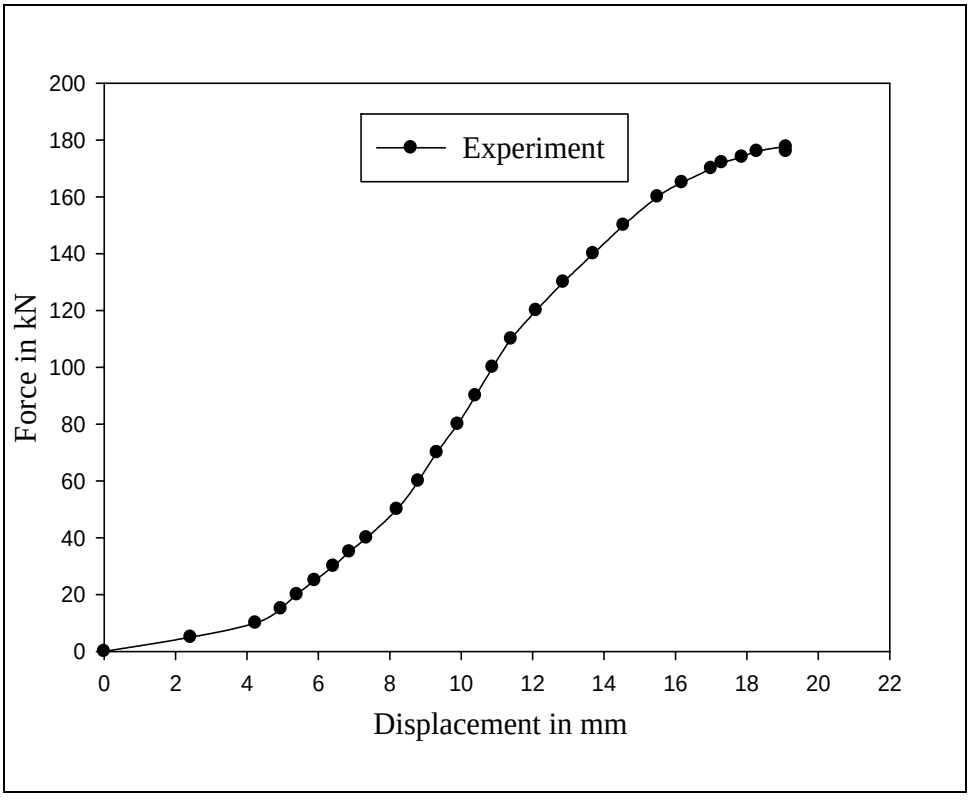

Fig. 3.12: Graph between force and displacement for specimen WT 3

- **SPECIMEN WT 4**:

Table 3.5: Experiment results for specimen WT 4

EXPERIMENT WT 4			
FORCE (kN)	DISPLACEMENT (mm)	STRESS (MPa)	STRAIN
0.00	0.00	0	0.0000
5.00	1.34	5	0.0017
10.00	2.44	10	0.0033
15.00	3.45	15	0.0052
20.00	4.20	20	0.0064
25.00	4.80	25	0.0073
30.00	5.50	30	0.0080
35.00	6.18	35	0.0088
40.00	6.83	40	0.0094
45.00	7.51	45	0.0104
50.00	8.10	50	0.0113
55.00	8.68	55	0.0122
60.00	9.20	60	0.0130
65.00	9.70	70	0.0143
70.00	10.14	80	0.0157
75.00	10.57	90	0.0167
80.00	11.16	100	0.0182
85.00	11.60	110	0.0193
90.00	12.05	115	0.0200
95.00	12.52	120	0.0209
100.00	13.11	125	0.0217
105.00	13.80	130	0.0224
110.00	14.35	135	0.0233
113.00	14.80	140	0.0241
115.00	15.00	143	0.0254
117.00	15.30	144	0.0259
119.10	16.10	140	0.0265
117.00	16.55	143	0.0263
113.00	16.75	135	0.0269

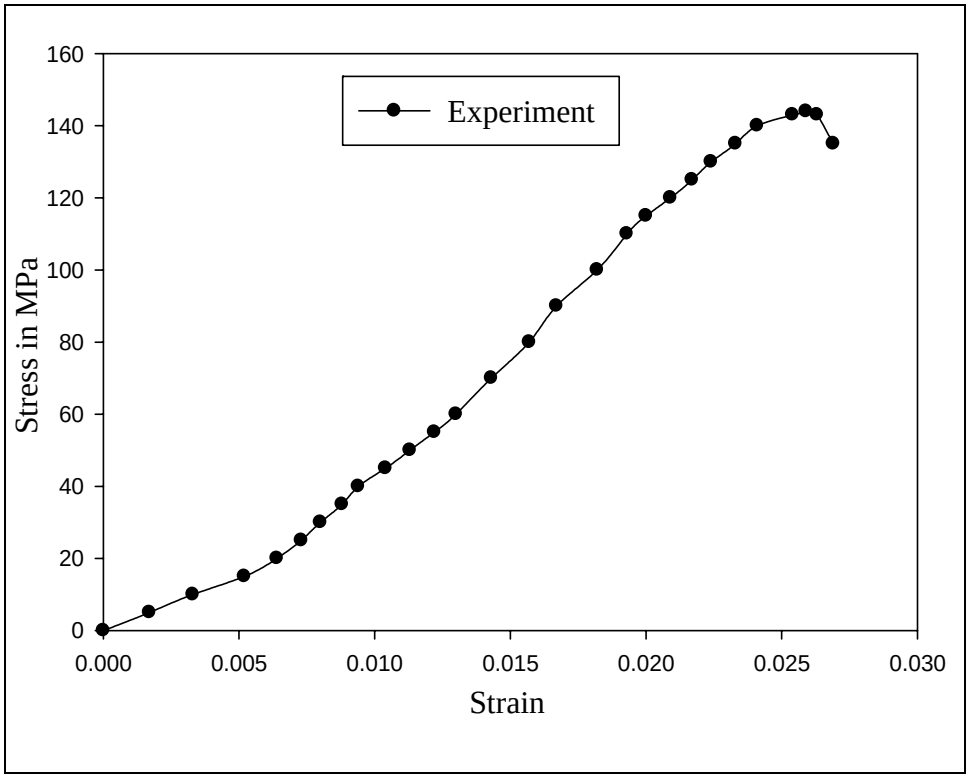

Fig. 3.13: Graph between stress and strain for specimen WT 4

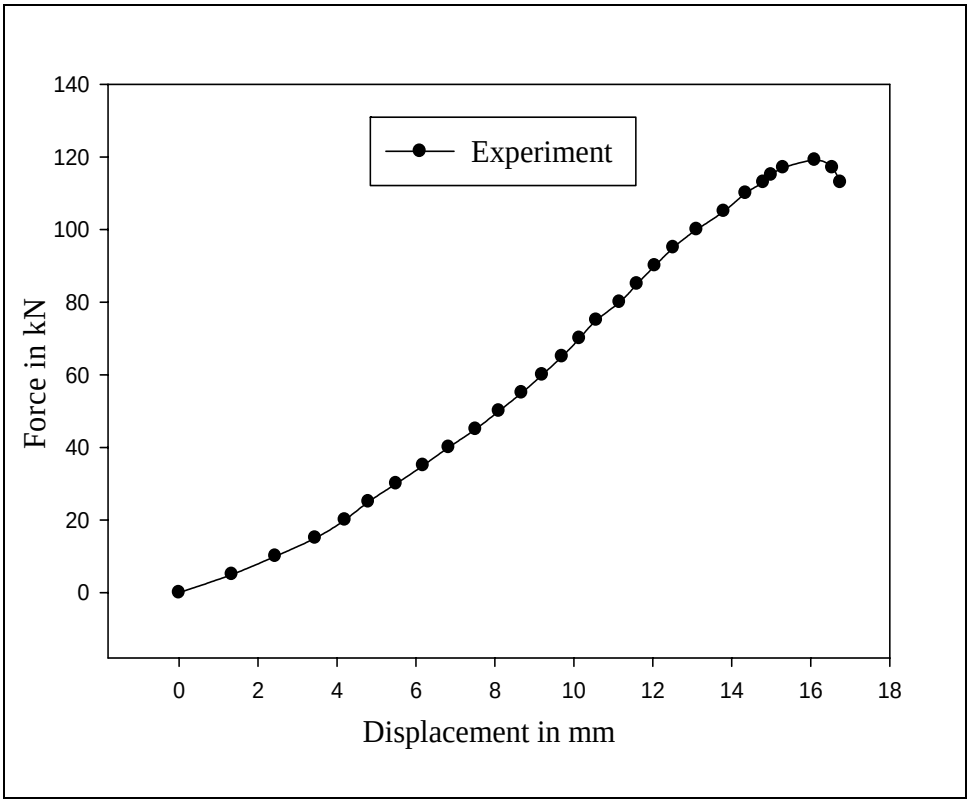

Fig. 3.14: Graph between force and displacement for specimen WT 4

- **SPECIMEN WT 5**:

Table 3.6: Experiment results for specimen WT 5

EXPERIMENT WT 5			
FORCE (kN)	DISPLACEMENT (mm)	STRESS (MPa)	STRAIN
0.00	0.00	0	0.0000
5.00	1.95	5	0.0048
10.00	3.50	10	0.0075
15.00	4.55	15	0.0089
20.00	5.52	20	0.0100
25.00	6.18	25	0.0106
30.00	6.83	30	0.0116
35.00	7.40	40	0.0127
40.00	8.20	50	0.0138
45.00	8.80	60	0.0146
50.00	9.30	70	0.0154
60.00	9.98	80	0.0162
70.00	10.68	90	0.0170
80.00	11.20	100	0.0180
90.00	11.92	110	0.0187
100.00	12.45	120	0.0196
110.00	13.10	130	0.0206
120.00	13.88	140	0.0213
130.00	14.55	150	0.0222
140.00	15.45	160	0.0232
150.00	16.20	170	0.0245
160.00	16.90	180	0.0255
170.00	17.50	190	0.0266
180.00	18.15	200	0.0280
190.00	18.72	210	0.0291
193.00	19.50	220	0.0309
190.00	20.20	224	0.0318
180.00	20.65	220	0.0324

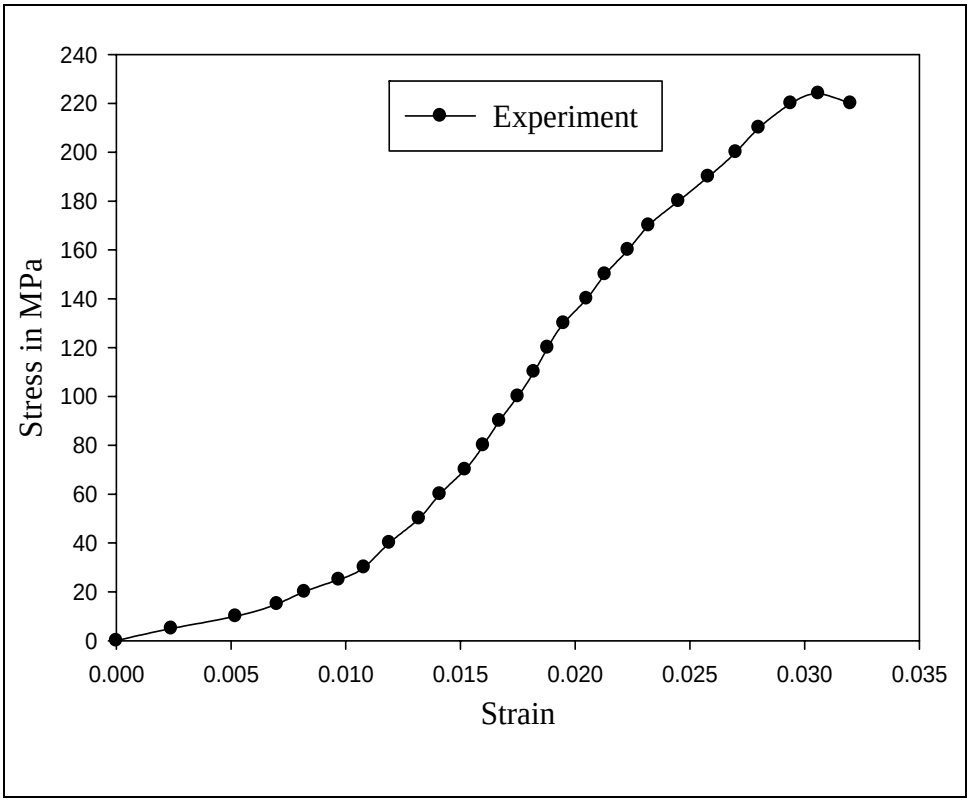

Fig. 3.15: Graph between stress and strain for specimen WT 5

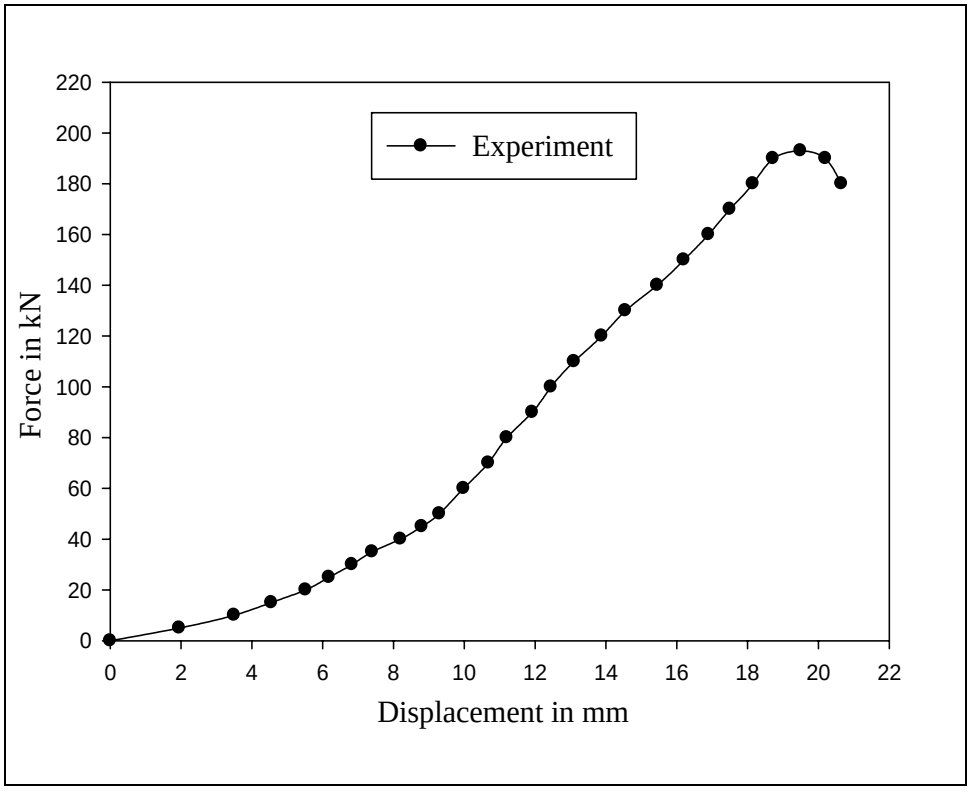

Fig. 3.16: Graph between force and displacement for specimen WT 5

- **SPECIMEN WT 6**:

Table 3.7: Experiment results for specimen WT 6

EXPERIMENT WT 6			
FORCE (kN)	DISPLACEMENT (mm)	STRESS (MPa)	STRAIN
0.00	0.00	0	0.0000
5.00	2.00	10	0.0039
10.00	3.60	20	0.0072
20.00	4.50	30	0.0094
30.00	6.00	40	0.0109
40.00	7.18	50	0.0120
50.00	8.00	60	0.0130
60.00	8.85	70	0.0140
70.00	9.28	80	0.0147
80.00	9.74	90	0.0152
90.00	10.30	100	0.0159
100.00	10.74	110	0.0164
110.00	11.30	120	0.0172
120.00	11.94	130	0.0180
130.00	12.45	140	0.0186
140.00	13.05	150	0.0192
150.00	13.90	160	0.0201
160.00	14.45	170	0.0208
170.00	15.23	180	0.0219
180.00	16.30	190	0.0226
190.00	17.25	200	0.0240
200.00	18.44	210	0.0250
204.00	18.86	220	0.0262
208.00	19.56	230	0.0273
212.00	20.30	240	0.0288
215.65	21.34	250	0.0307
212.00	22.50	260	0.0326
208.00	22.73	262	0.0341
204.00	23.20	260	0.0356

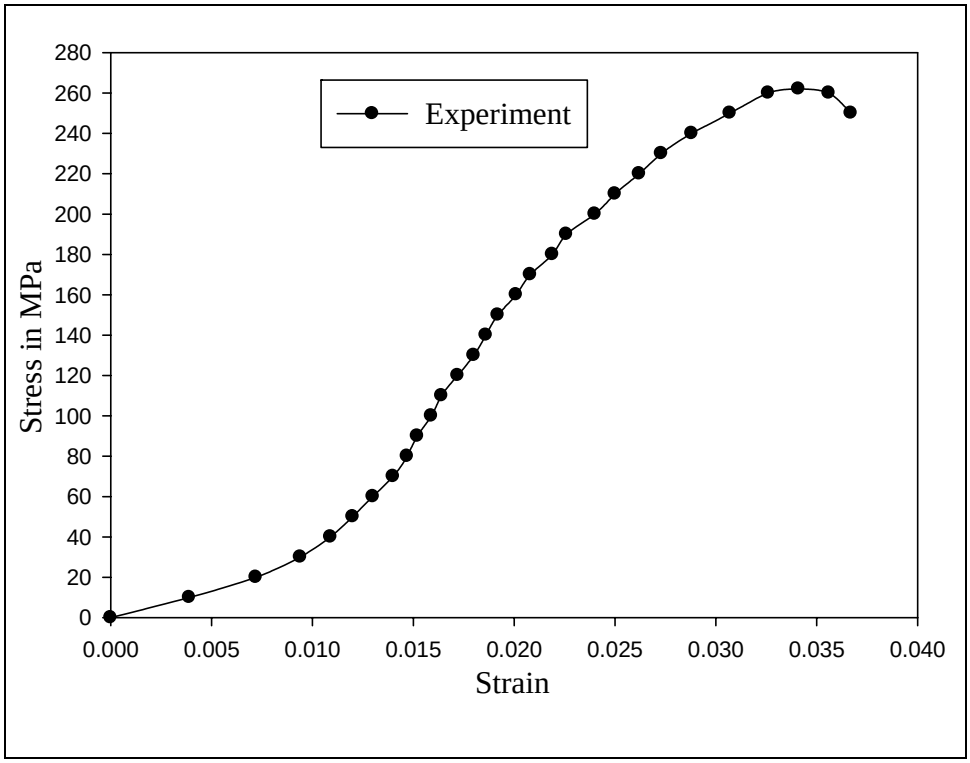

Fig. 3.17: Graph between stress and strain for specimen WT 6

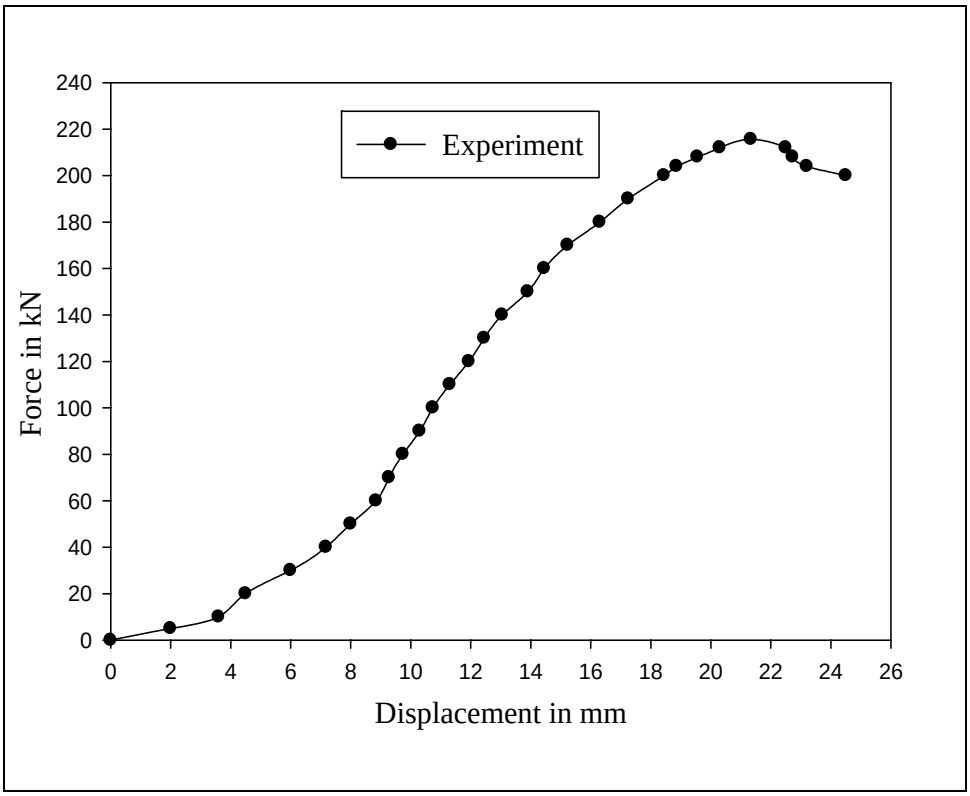

Fig. 3.18: Graph between force and displacement for specimen WT 6

3.5 SPECIMEN MODE OF FAILURES

The typical specimen failures (specimens: WT1, WT 2, WT 3, WT 4, WT 5 and WT 6) consisted of a partial rupturing of the net section. Tests were stopped when the peak load was reached. The peak load was reached before fracturing of the full net section, but after rupture of the partial net section. Fracturing of a specimen's web initiated at the lead bolt hole and propagated to the web's outside edge. Necking down of the tension plane area preceded fracture. Specimens with small eccentricities exhibited a significant amount of bolt hole deformation (shown in Fig. 3.19). However, it was observed that the amount of deformation decreased with increasing eccentricity. Those specimen with the largest eccentricities demonstrated very minor hole deformation except at the lead and last bolts (shown in Fig. 3.20).

Fig. 3.19: Partial net section rupture, with small eccentricity (specimen 6)

Fig. 3.20: Partial net section rupture, with large eccentricity (specimen 4)

3.6 EFFECTS OF CONNECTION ECCENTRICITY

Eccentricity is readily observed to have a direct impact on a connection's net section efficiency. Table 3.9 clearly shows that as connection eccentricity decreases, there is a increase in member efficiency for the three bolt connection specimens.

The inconsistencies between LRFD predictions and the failure loads may be attributed to primary bending moments' resulting from connection eccentricity, which is not accounted for in present specifications. The effects of an axial load will be increased because of an eccentricity induced flexural load. This will have the greatest affect on the web, causing a premature rupture of the partial net section area. Fig. 3.21 shows a specimen subjected to a loading of "P" acting at the connection. Using statics, the resulting internal forces of a body can be reduced to a force and moment acting at some location. The resultant internal force acts through the centroidal axis of the member. However, because the external and resultant internal force are not in the same line of action an internal moment is produced, which is equal to the distance between the two forces (the in-plane eccentricity, " *x* ") multiplied by the magnitude of the moment couple (the applied external load, "P"). Therefore, the eccentricities should properly be accounted for in the design equations, but are not.

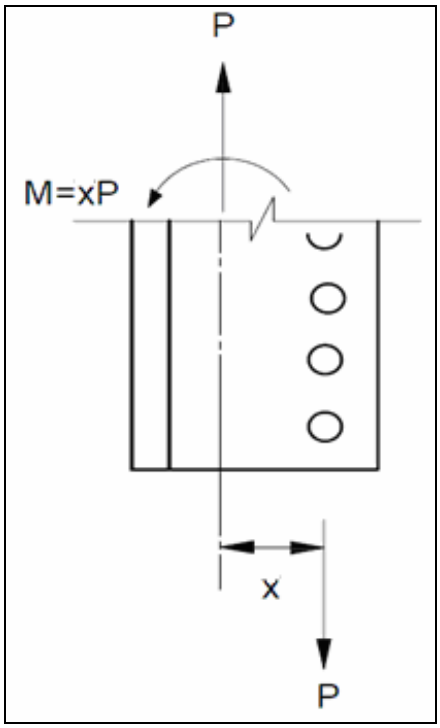

Fig. 3.21: Primary bending moments resulting from connection eccentricity

To reduces the detrimental effects of bending restoring moment being developed at the connection. It is a function of connection length and the in-plane stiffness of the bar stock grips (typical of gusset plates). Hence, the failure load of the specimen exceeds the interaction equation prediction. Fig. 3.22 shows the beneficial effect of the restoring moment.

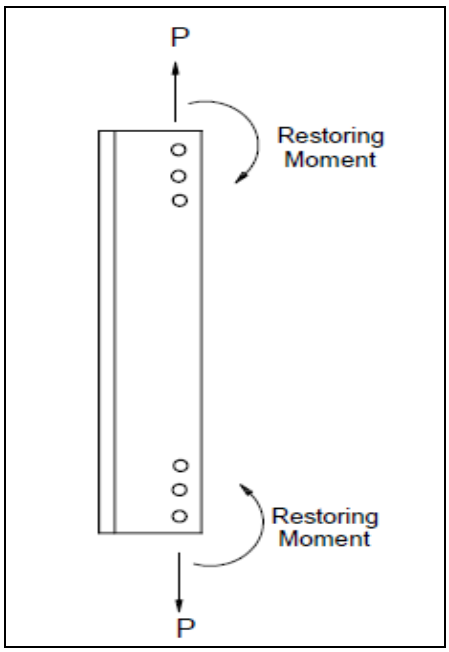

Fig. 3.22: Restoring moment developed as a function of connection restraint

3.7 EFFECTS OF CONNECTION LENGTH

The net section efficiency of the specimens tested increased by an average of 9-11% when the connection length was increased from 100 mm to 150 mm by increasing the pitch as shown in Table 3.9.

The increases in net section efficiency shown here are due possibly to two benefits of increased connection length.

First, a possible benefit to a longer connection length is that it allows shear lag effects to be reduced.

Secondly, an increase in the connection length of a specimen allows for a larger restoring moment at the connection. The connection length limits the restoring moment's lever-arm. A longer connection length permits, therefore, a larger restoring moment to develop, increasing net section efficiency.

3.8 AISC LRFD PREDICTIONS

A comparison of these experimental results with the LRFD predictions was done. All the values calculated according to the specification, which are presented in Table 3.9, are calculated without the inclusion of any resistance factors. The bearing strengths are calculated on the assumption that bolt hole deformation is not a concern. All bolts, because of the pair of bar stock grips fastened at either end of a specimen, are subjected to double shear. The area calculations of all the specimens which are used to calculate AISC-LRFD limit states are presented in Table 3.8. A sample calculation of specimens WT 1 for each of the LRFD limit states and a form of the LRFD interaction equation, are given below.

Table 3.8: Specimen area calculations

Spec. No.	Gross cross sectional area, Ag (mm^2)	Net cross sectional area, An (mm^2)	Gross tension plane area, Agt (mm^2)	Net tension plane area, Ant (mm^2)	Gross shear plane area, Agv (mm^2)	Net shear plane area, Anv (mm^2)
WT-1	822	758	80	48	568	408
WT-2	822	758	128	96	568	408
WT-3	822	758	176	144	568	408
WT-4	822	758	80	48	768	608
WT-5	822	758	128	96	768	608
WT-6	822	758	176	144	768	608

Table 3.9: Specimen Failure Loads and Predicted Capacities (PNS=Partial net section rupture)

Spec. No.	Exp. Load	Spec. Failure Type	AISC-LRFD Limit States (kN)						AISC Pred Capacity	Prof. Factor $\frac{P_{exp}}{P_{aisc}}$	FuAnet	Efficiency $\frac{P_{exp}}{F_u A_{net}}$
			Rupture		Yielding	Bolt Bearing	Bolt Shear (double)	Block Shear				
			Calc.	Max.								
WT1	117.2	PNS	179.2	348.7	205.5	248.4	519.5	132.6	132.6	0.88	348.7	0.34
WT2	175.0	PNS	221.0	348.7	205.5	248.4	519.5	144.6	144.6	1.21	348.7	0.50
WT3	177.5	PNS	262.9	348.7	205.5	248.4	519.5	156.6	156.6	1.13	348.7	0.51
WT4	119.1	PNS	235.7	348.7	205.5	248.4	519.5	187.8	187.8	0.63	348.7	0.35
WT5	206.4	PNS	263.6	348.7	205.5	248.4	519.5	199.8	199.8	1.03	348.7	0.59
WT6	215.6	PNS	291.5	348.7	205.5	248.4	519.5	211.8	205.5	1.05	348.7	0.62

Gross Section Yielding

$$P_n = F_y A_g \qquad \text{[LRFD (D1-1)]}$$

$$P_n = (250MPa).\left(\frac{822mm^2}{10^3}\right) = 205.5kN$$

Net Section Rupture

$$P_n = F_u A_e \qquad \text{[LRFD (D1-2)]}$$

Where $A_e = UA_{net}$

$$U = 1 - \frac{x}{L} = 1 - \frac{48.61}{100} = 0.514 \qquad \text{[LRFD, (B3-2)]}$$

$$A_e = 0.51 \times 758 = 389.53mm^2 \qquad \text{[LRFD, (B3-1)]}$$

$$P_n = (460MPa).\left(\frac{389.53mm^2}{10^3}\right) = 179.18kN$$

Block Shear [LRFD, J4.3]

Where:

$$A_{gt} = t.(d - g) = (4mm).(90mm - 70mm) = 80mm^2$$

$$A_{nt} = A_{gt} - 0.5d_h.t = 80mm^2 - 0.5 \times 16mm \times 4mm = 48mm^2$$

$$A_{gv} = t.(L + 42mm) = 4.(100mm + 42mm) = 568mm^2$$

$$A_{nv} = A_{gv} - 2.5d_h.t = 568mm - 2.5 \times 16mm \times 4mm = 508mm^2$$

d_h = *hole diameter*

$$F_u A_{nt} = 460MPa \times \frac{48mm^2}{10^3} = 22.08kN \le 0.6F_u A_{nv} = 0.6 \times 460MPa \times \frac{440mm^2}{10^3} = 121.44kN$$

Therefore, LRFD Eqn. (J4-3b) controls

$$R_n = F_y A_{gt} + 0.6F_u A_{nv} = \left(250MPa \times \frac{80mm^2}{10^3}\right) + \left(0.6 \times 460MPa \times \frac{440mm^2}{10^3}\right) = 141.44kN$$

Bolt Bearing [LRFD, (J3-1b)]

$$R_n = 3.0d_b.t.F_u n = 3.0.\left(\frac{15mm \times 4mm}{10^3}\right) \times 460MPa \times 3 = 248.4kN$$

Where d_b =*bolt diameter*

Bolt Shear [LRFD, J3.6]

$$R_n = \tau.A_b.m.n = 490MPa.\left(\frac{176.78mm^2}{10^3}\right).2\times 3 = 519.75kN$$

CHAPTER 4
FINITE ELEMENT ANALYSIS

4.1 GENERAL

The goal of the Finite Element Analysis was to develop a model that could study the effect of connection eccentricity and connection length on WT tension member. In order to test the validity, the results obtained from the analysis were used to compare with the test results from the experiments. The Finite Element Analysis was performed using the commercial Finite Element Program ANSYS, version 11.0.

4.2 FINITE ELEMENT ANALYSIS

The main objective of the FEA is not only to estimate the failure loads of the WT section specimens but also to trace the entire load versus deflection path. The FEA is performed using 3D solid elements. A four node tetrahedral element (ANSYS Solid 185) was used in the Finite Element modeling of the WT section. The gusset plate was modeled using eight node hexahedral element (ANSYS Solid 185). The size of the element was taken as 8mm for both WT specimen and gusset plates. The WT specimen used in ANSYS are shown in Fig. 3.1 and Fig. 3.2 of Chapter 3. The WT specimen grip assembly used in ANSYS is shown in Fig.3.6 of Chapter 3.

In the finite element model, a surface-to-surface contact is used to fully transfer the load from the gusset plate to the web. That is, a surface-to-surface contact option is used between the bolt's outer surface and the inner surface of the web holes. Additionally, a surface contact option is also used between the bolt's outer surface and the inside surface of the gusset plate holes. Similarly, a surface contact option is applied between the bottom surface of the gusset plate and the top surface of the web in order to avoid gap between the gusset plate and the web. The bottom side of the two lower gusset plates was fixed and the load was applied on the top side of the upper two gusset plates. The typical mesh used in the Finite Element Analysis is shown in Fig. 4.1. Fig. 4.2 shows the stress (MPa) and strain contour for specimen WT 1.

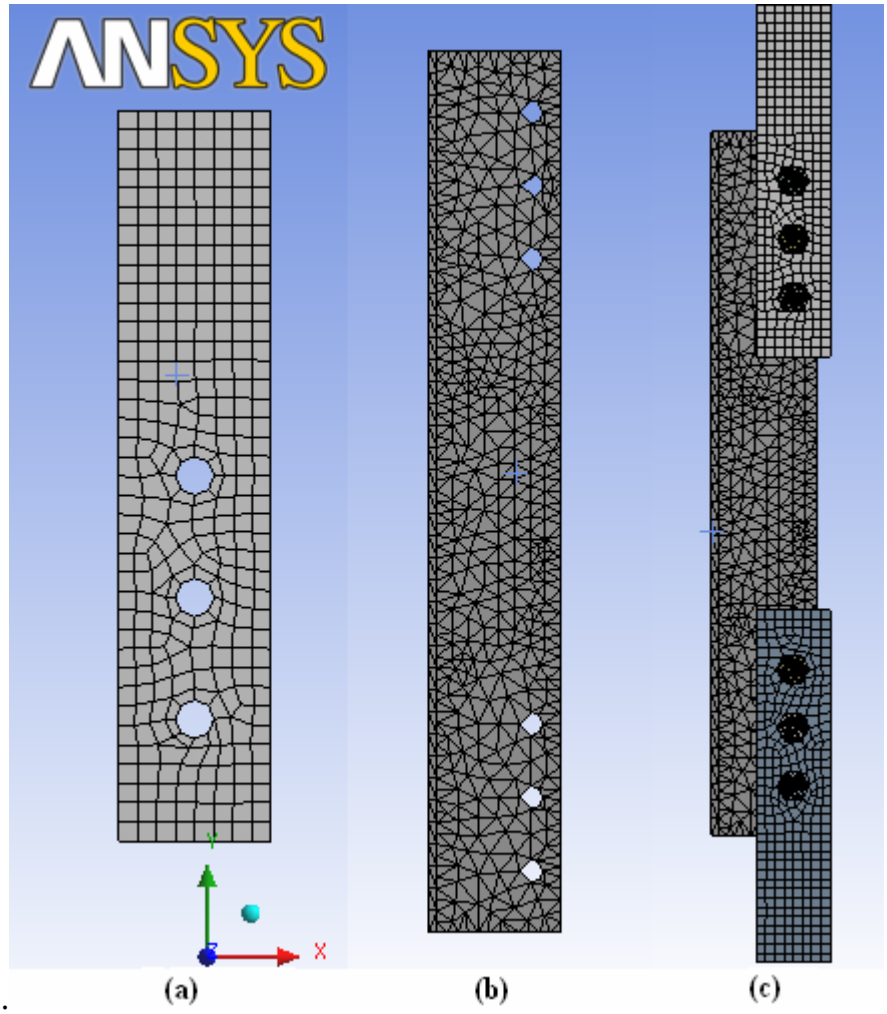

Fig. 4.1: Typical Finite Element mesh (a) Gusset plate (b) WT specimen (c) Full assembly

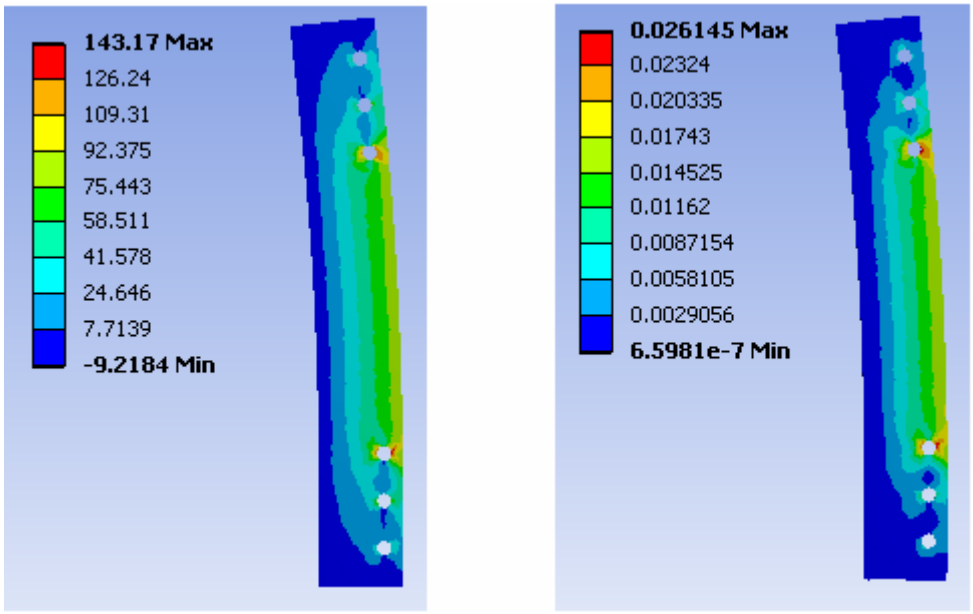

Fig. 4.2: Stress contour and strain contour of specimen WT 1

The results obtained from the FEA are detailed below:

- **SPECIMEN WT 1**:

Table 4.1: Simulation results for specimen WT 1

SIMULATION WT 1			
FORCE (kN)	DISPLACEMENT (mm)	STRESS (MPa)	STRAIN
0.00	0.00	0.00	0.0000
5.00	1.12	5.05	0.0013
10.00	2.08	9.56	0.0027
15.00	2.87	14.51	0.0038
20.00	3.58	19.26	0.005
25.00	4.28	26.25	0.0062
30.00	4.95	30.25	0.0071
35.00	5.58	35.00	0.0081
40.00	6.15	40.58	0.0091
45.00	6.73	45.21	0.0100
50.00	7.28	49.62	0.0108
55.00	7.89	58.13	0.0123
60.00	8.42	69.50	0.0137
65.00	9.08	80.15	0.0151
70.00	9.68	90.35	0.0165
75.00	10.21	101.35	0.0182
80.00	10.70	109.87	0.0193
85.00	11.31	114.87	0.0200
90.00	11.92	121.25	0.0211
95.00	12.62	125.00	0.0216
100.00	13.25	130.25	0.0226
105.00	13.92	136.54	0.0239
110.00	14.59	139.26	0.0251
113.00	15.56	141.23	0.0255
115.00	15.95	142.32	0.0257
117.20	16.21	143.17	0.0261

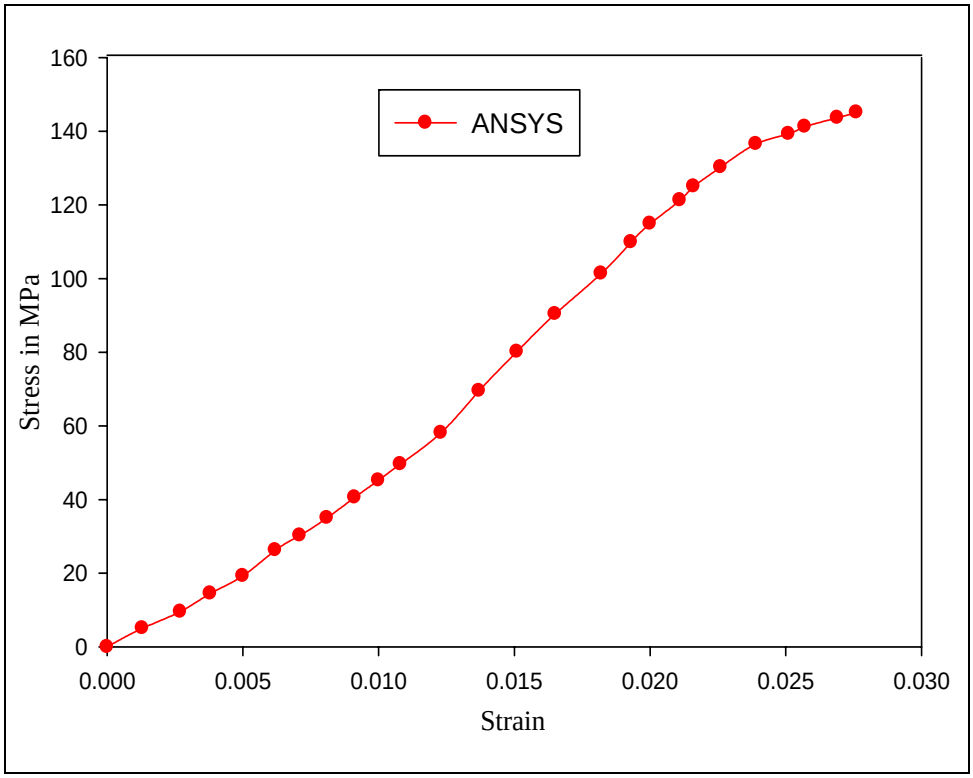

Fig. 4.3: Graph between stress and strain for specimen WT 1

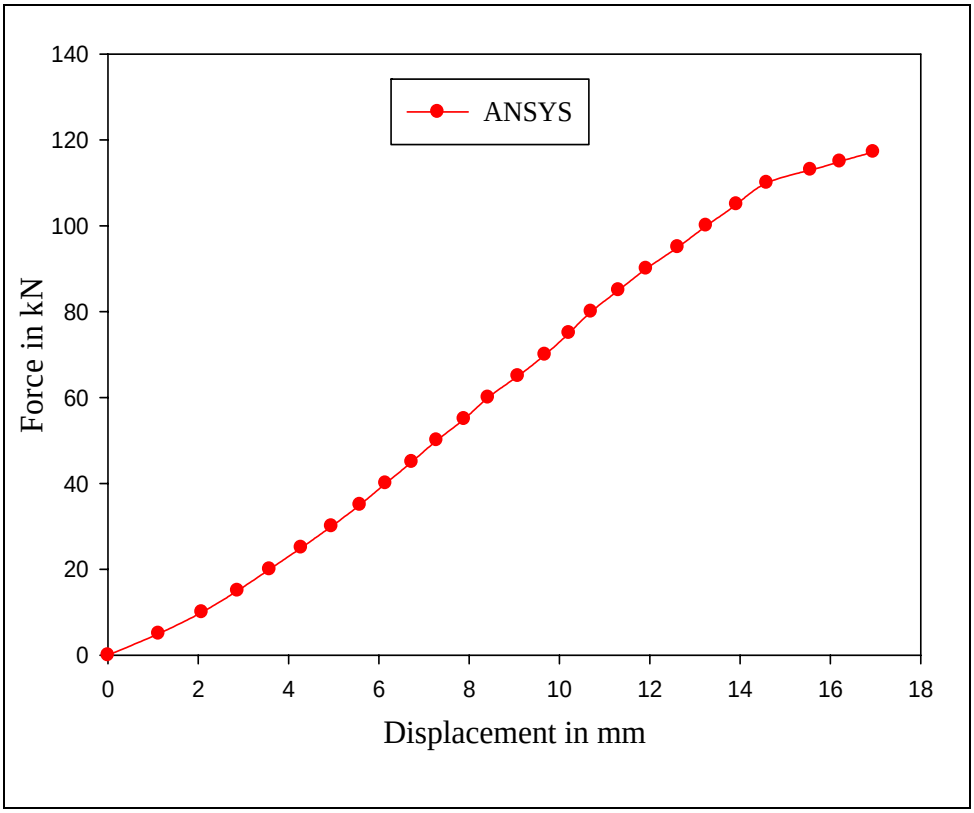

Fig. 4.4: Graph between force and displacement for specimen WT 1

- **SPECIMEN WT 2**:

Table 4.2: Simulation results for specimen WT 2

SIMULATION WT 2			
FORCE (kN)	DISPLACEMENT (mm)	STRESS (MPa)	STRAIN
0.00	0.00	0.00	0.0000
5.00	0.97	6.12	0.0012
10.00	1.84	10.58	0.0021
15.00	2.61	15.24	0.0031
20.00	3.28	20.04	0.0040
25.00	3.88	24.96	0.0051
30.00	4.41	29.85	0.0059
35.00	4.88	35.00	0.0069
40.00	5.43	40.25	0.0077
45.00	5.93	50.14	0.0090
50.00	6.43	59.23	0.0103
55.00	6.95	69.10	0.0115
60.00	7.51	81.25	0.0130
65.00	8.12	90.25	0.0140
70.00	8.70	102.57	0.0152
75.00	9.31	109.95	0.0160
80.00	9.82	120.45	0.0170
85.00	10.33	130.00	0.0181
90.00	10.89	140.65	0.0193
100.00	11.85	145.14	0.0201
110.00	12.77	150.65	0.0212
120.00	13.73	155.75	0.0225
130.00	14.76	160.00	0.0237
140.00	15.81	164.25	0.0245
150.00	17.08	168.32	0.0253
152.00	18.65	172.36	0.0271

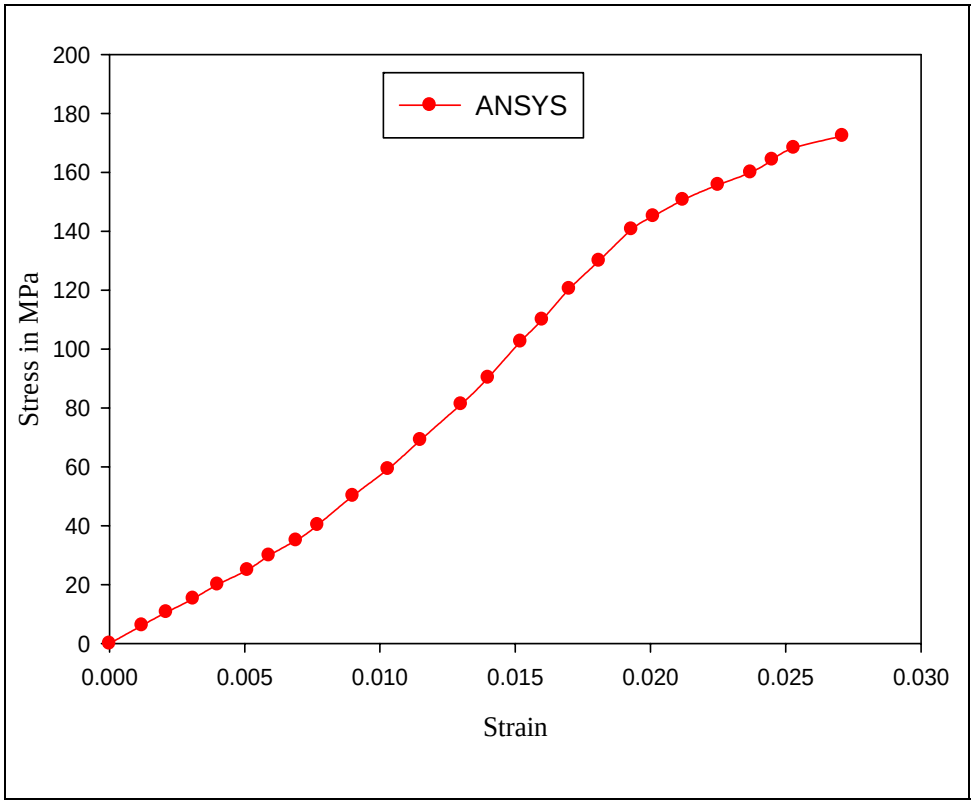

Fig. 4.5: Graph between stress and strain for specimen WT 2

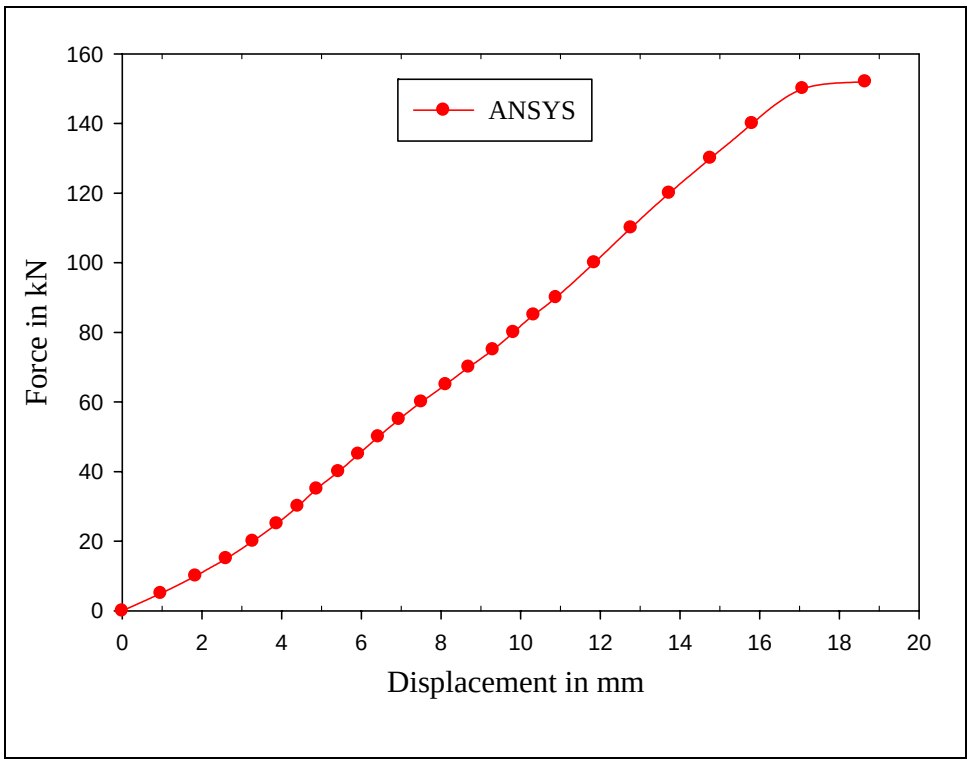

Fig. 4.6: Graph between force and displacement for specimen WT 2

- **SPECIMEN WT 3**:

Table 4.3: Simulation results for specimen WT 3

SIMULATION WT 3			
FORCE (kN)	DISPLACEMENT (mm)	STRESS (MPa)	STRAIN
0.00	0.00	0.00	0.0000
5.00	0.79	4.31	0.0012
10.00	1.67	10.56	0.0025
15.00	2.43	20.76	0.0047
20.00	3.27	31.25	0.0064
25.00	3.98	39.58	0.0075
30.00	4.61	48.85	0.0091
35.00	5.24	59.36	0.0104
40.00	5.87	70.12	0.0117
50.00	6.95	80.00	0.0128
60.00	7.92	90.65	0.0137
70.00	8.78	99.26	0.0146
80.00	9.64	112.56	0.0159
90.00	10.40	120.24	0.0164
100.00	11.20	129.34	0.0172
110.00	12.03	138.25	0.0181
120.00	12.85	148.12	0.0190
130.00	13.67	159.35	0.0202
140.00	14.23	170.05	0.0215
150.00	14.86	179.00	0.0225
160.00	15.35	189.36	0.0237
165.00	15.87	201.35	0.0255
170.00	16.15	206.45	0.0263
172.00	16.28	211.58	0.0280
174.00	16.54	215.50	0.0295
176.00	16.85	217.32	0.0309
177.50	17.32	218.56	0.0315

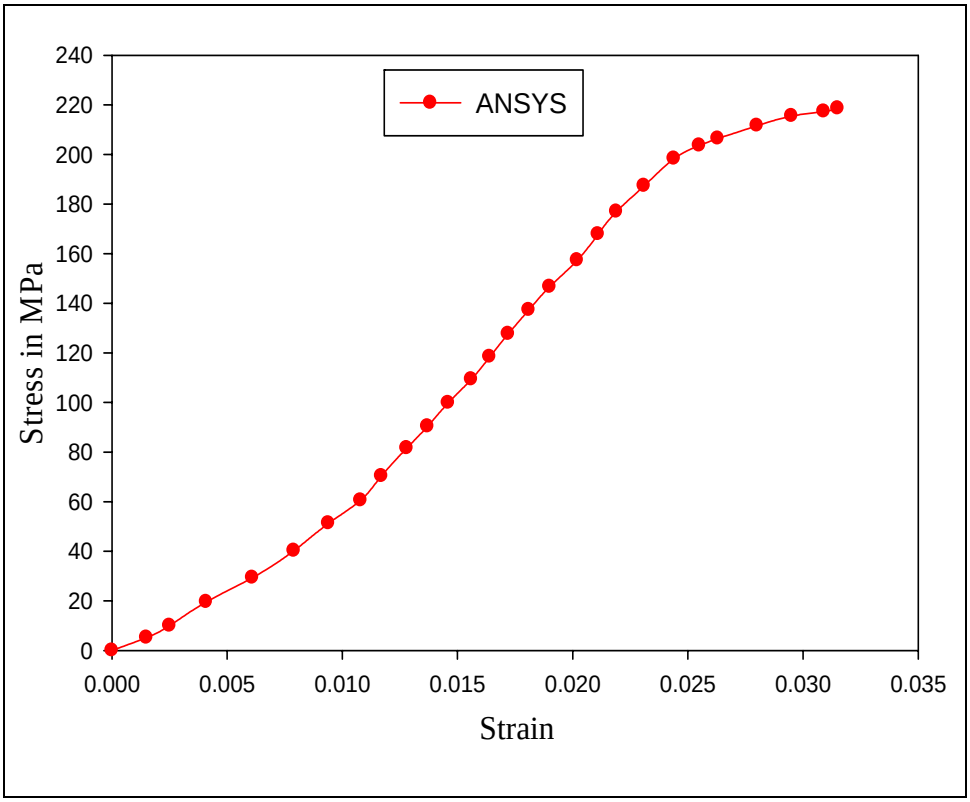

Fig. 4.7: Graph between stress and strain for specimen WT 3

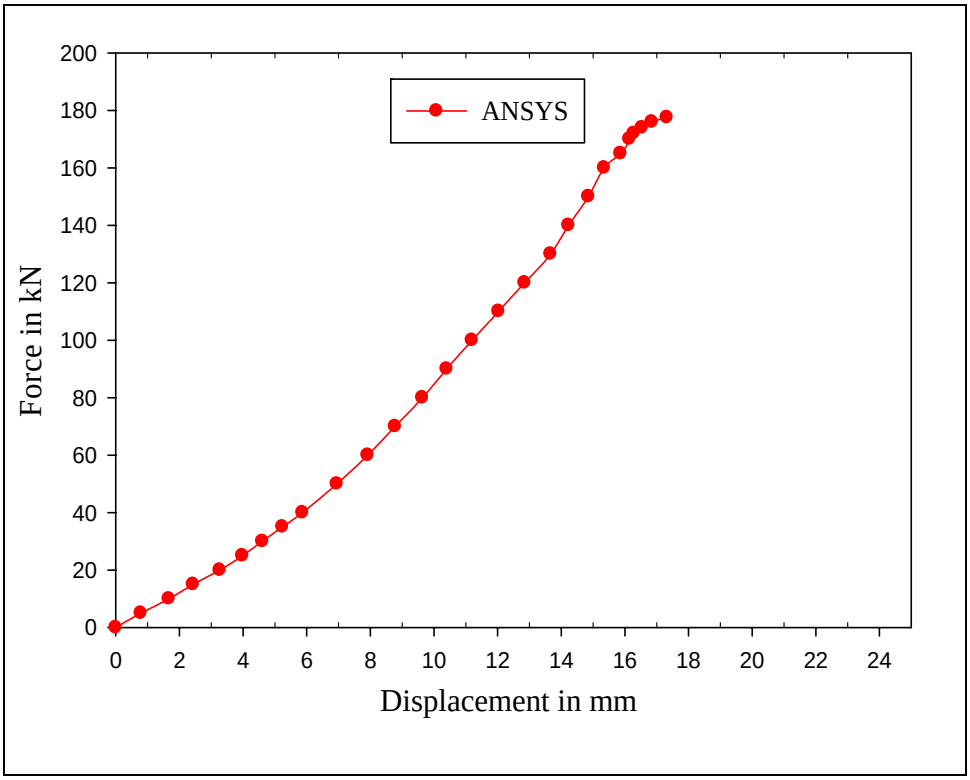

Fig. 4.8: Graph between force and displacement for specimen WT3

- **SPECIMEN WT 4**:

Table 4.4: Simulation results for specimen WT 4

SIMULATION WT 4			
FORCE (kN)	DISPLACEMENT (mm)	STRESS (MPa)	STRAIN
0.00	0.00	0.00	0.0000
5.00	1.15	5.13	00016
10.00	2.25	10.25	0.0027
15.00	3.23	14.95	0.0039
20.00	3.99	19.65	0.0049
25.00	4.59	25.00	0.0060
30.00	5.29	31.01	0.0071
35.00	5.98	35.50	0.0079
40.00	6.63	39.97	0.0087
45.00	7.27	46.05	0.0096
50.00	7.87	50.67	0.0105
55.00	8.54	55.00	0.0113
60.00	9.04	60.04	0.0121
65.00	9.56	71.36	0.0137
70.00	10.03	79.25	0.0147
75.00	10.65	92.05	0.0166
80.00	11.21	98.82	0.0176
85.00	11.71	104.28	0.0182
90.00	12.16	115.31	0.0197
95.00	12.66	120.04	0.0203
100.00	13.22	125.25	0.0212
105.00	13.65	131.65	0.0218
110.00	14.23	137.35	0.0226
113.00	14.52	142.10	0.0232
115.00	15.01	144.32	0.0237
117.00	15.25	147.13	0.0246
119.10	15.75	148.35	0.0251

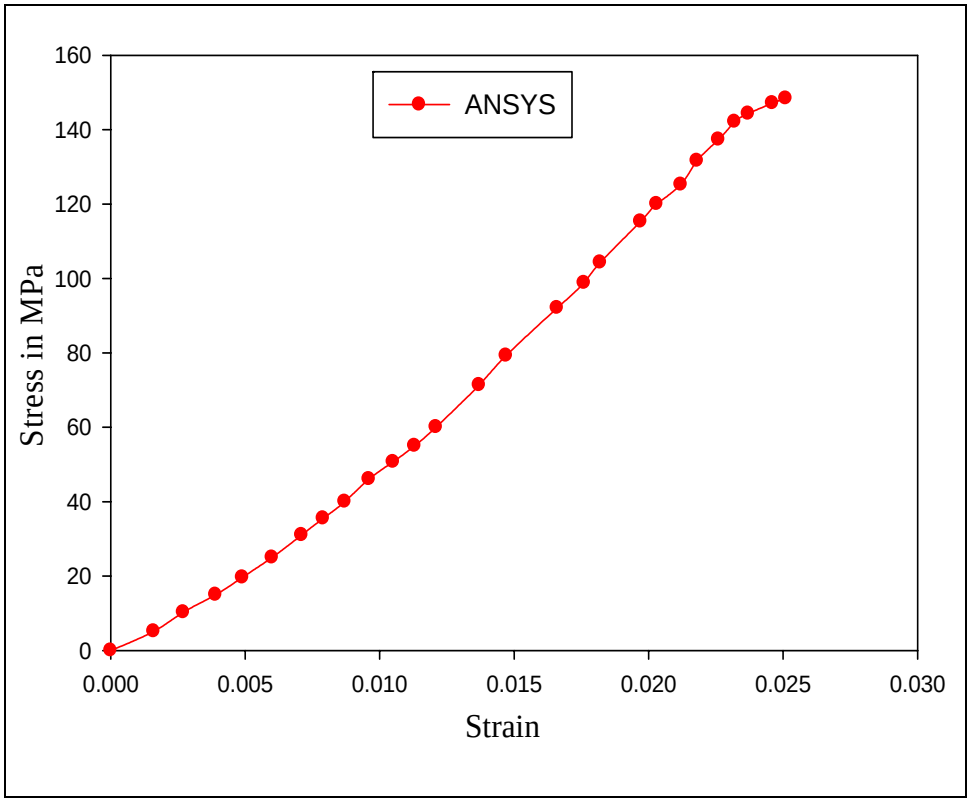

Fig. 4.9: Graph between stress and strain for specimen WT 4

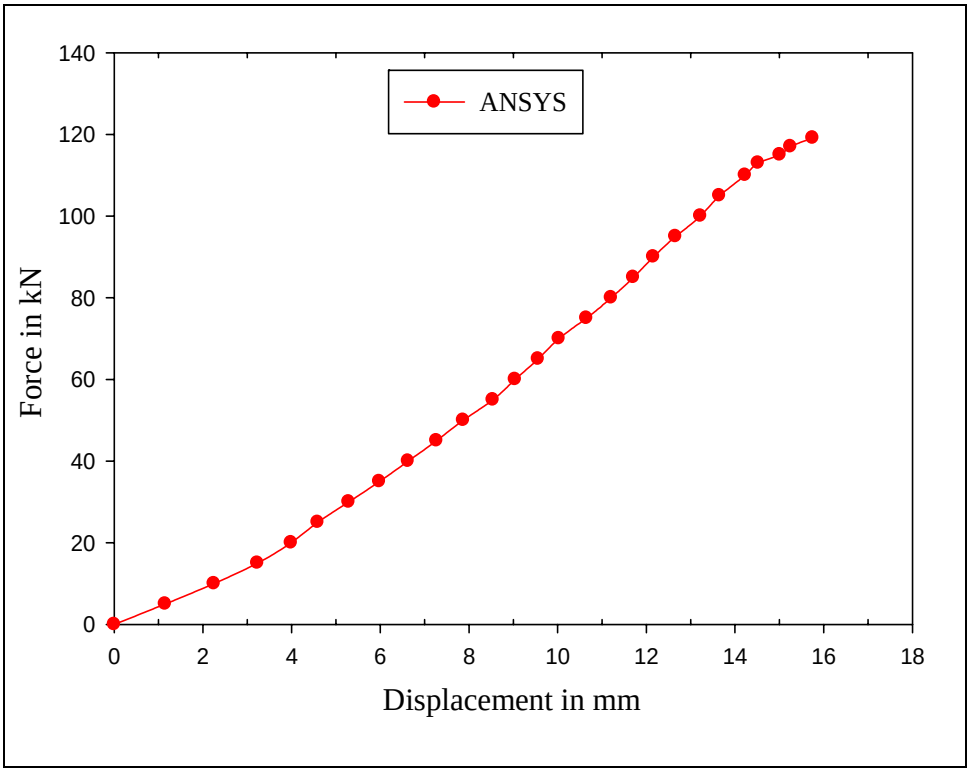

Fig. 4.10: Graph between force and displacement for specimen WT 4

- **SPECIMEN WT 5**:

Table 4.5: Simulation results for specimen WT51

SIMULATION WT 1			
FORCE (kN)	DISPLACEMENT (mm)	STRESS (MPa)	STRAIN
0.00	0.00	0.00	0.0000
5.00	1.01	4.32	0.0011
10.00	2.24	8.63	0.0023
15.00	3.36	14.32	0.0035
20.00	4.36	18.98	0.0046
25.00	5.15	25.00	0.0054
30.00	5.78	30.25	0.0064
35.00	6.60	40.85	0.0082
40.00	7.23	51.35	0.0096
45.00	7.89	60.21	0.0108
50.00	8.41	69.65	0.0123
60.00	9.43	79.25	0.0135
70.00	10.33	88.65	0.0145
80.00	11.21	98.23	0.0158
90.00	12.03	109.62	0.0170
100.00	12.70	120.25	0.0181
110.00	13.47	131.57	0.0191
120.00	14.18	142.63	0.0203
130.00	14.98	151.65	0.0212
140.00	15.71	160.00	0.0220
150.00	16.52	170.35	0.0229
160.00	17.31	180.24	0.0238
170.00	17.92	192.25	0.0248
180.00	18.70	202.35	0.0259
190.00	19.42	213.25	0.0274
193.00	20.38	221.65	0.0289

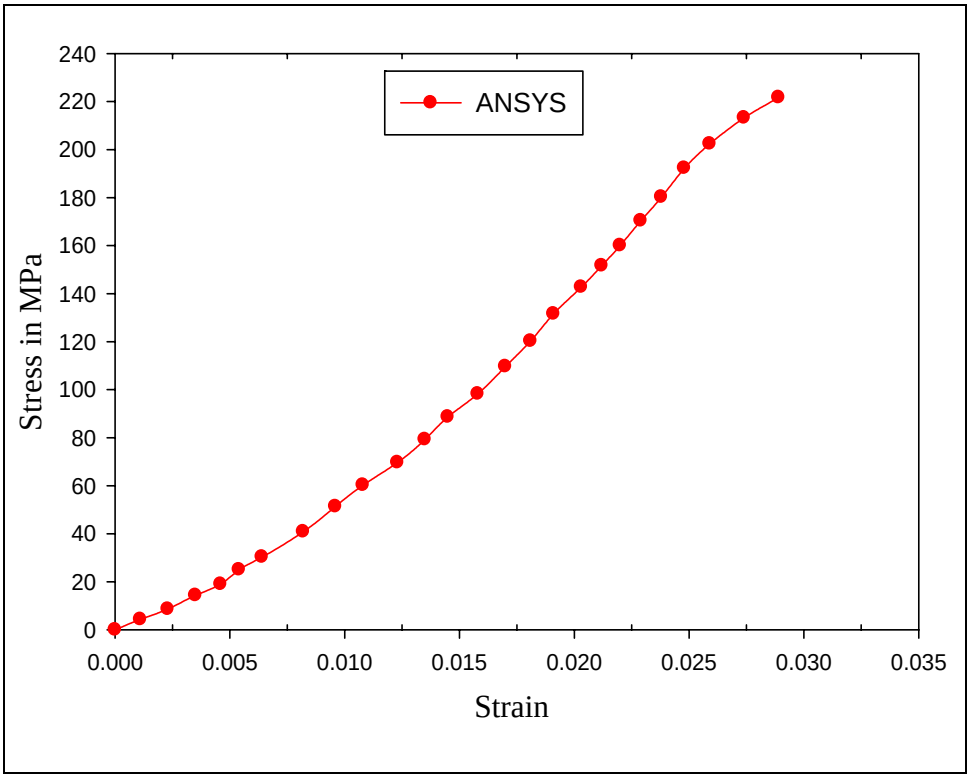

Fig. 4.11: Graph between stress and strain for specimen WT 5

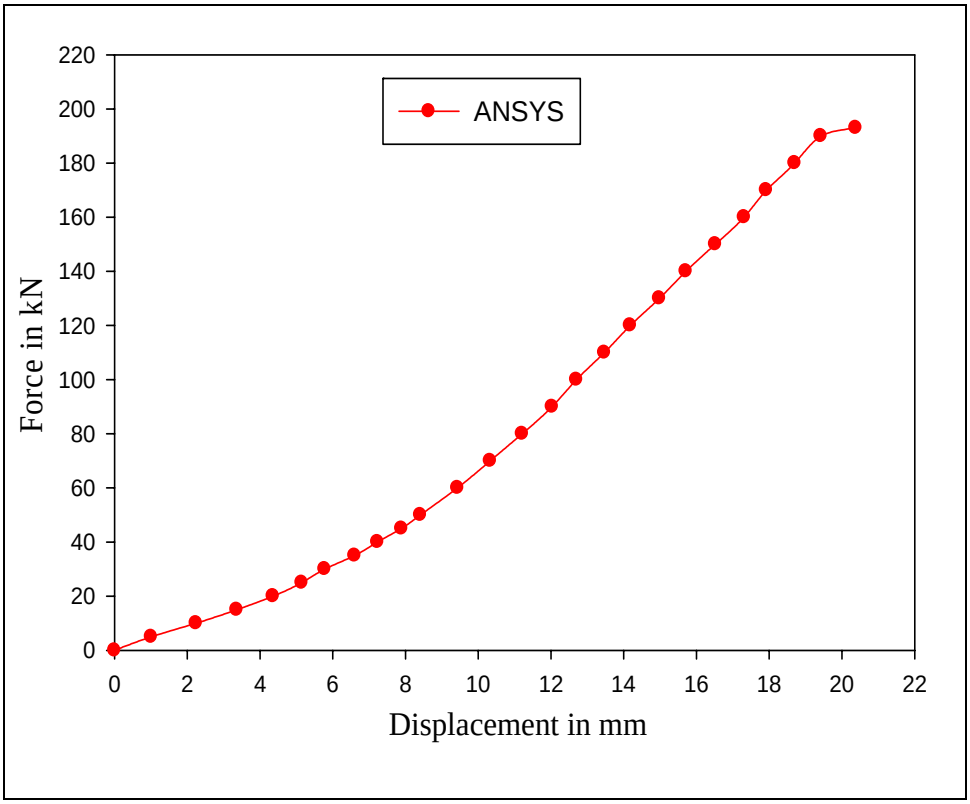

Fig. 4.12: Graph between force and displacement for specimen WT 5

- **SPECIMEN WT 6**:

Table 4.6: Simulation results for specimen WT 6

SIMULATION WT 6			
FORCE (kN)	DISPLACEMENT (mm)	STRESS (MPa)	STRAIN
0.00	0.00	0.00	0.0000
5.00	0.85	8.50	0.0018
10.00	1.51	19.00	0.0036
20.00	2.62	30.45	0.0055
30.00	3.71	38.56	0.0068
40.00	4.82	50.00	0.0083
50.00	5.85	59.60	0.0097
60.00	6.64	71.25	0.0109
70.00	7.58	79.65	0.0119
80.00	8.56	90.00	0.0130
90.00	9.35	100.56	0.0139
100.00	10.25	108.52	0.0148
110.00	11.11	117.56	0.0156
120.00	11.77	129.56	0.0165
130.00	12.64	140.68	0.0175
140.00	13.25	150.00	0.0183
150.00	13.90	160.25	0.0192
160.00	14.55	169.24	0.0201
170.00	15.30	178.58	0.0211
180.00	15.91	189.85	0.0222
190.00	16.92	202.56	0.0234
200.00	17.74	209.35	0.0243
204.00	18.35	218.36	0.0255
208.00	18.98	228.34	0.0264
212.00	19.54	238.66	0.0276
215.65	19.99	247.65	0.0287
216.00	20.65	257.10	0.0301

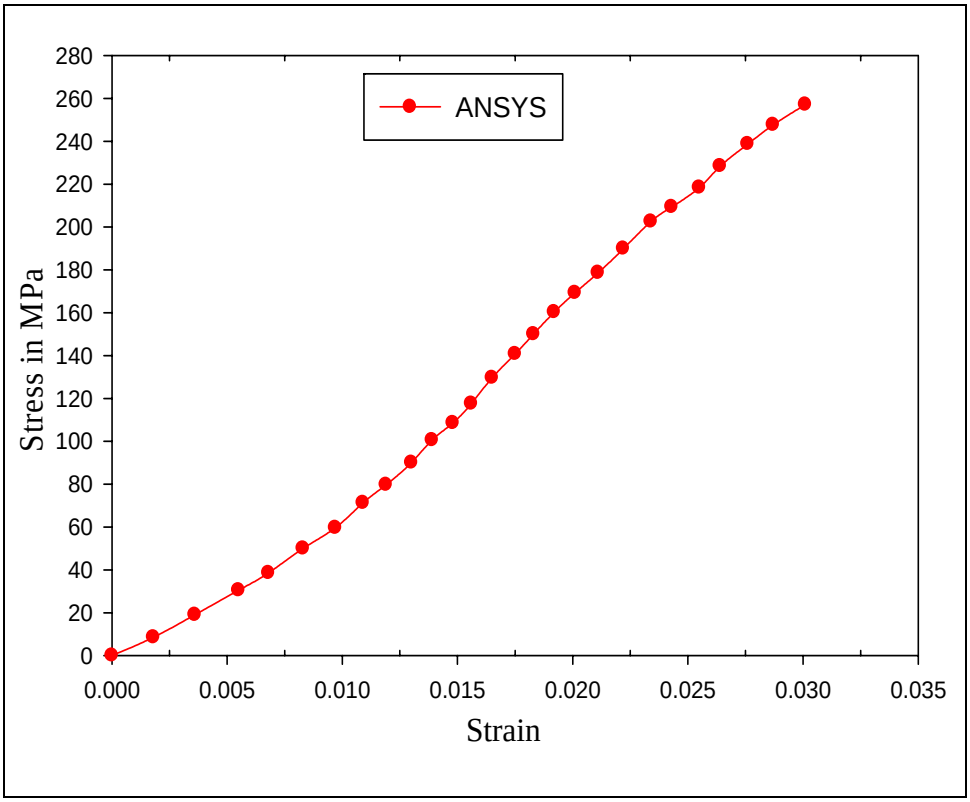

Fig. 4.13: Graph between stress and strain for specimen WT6

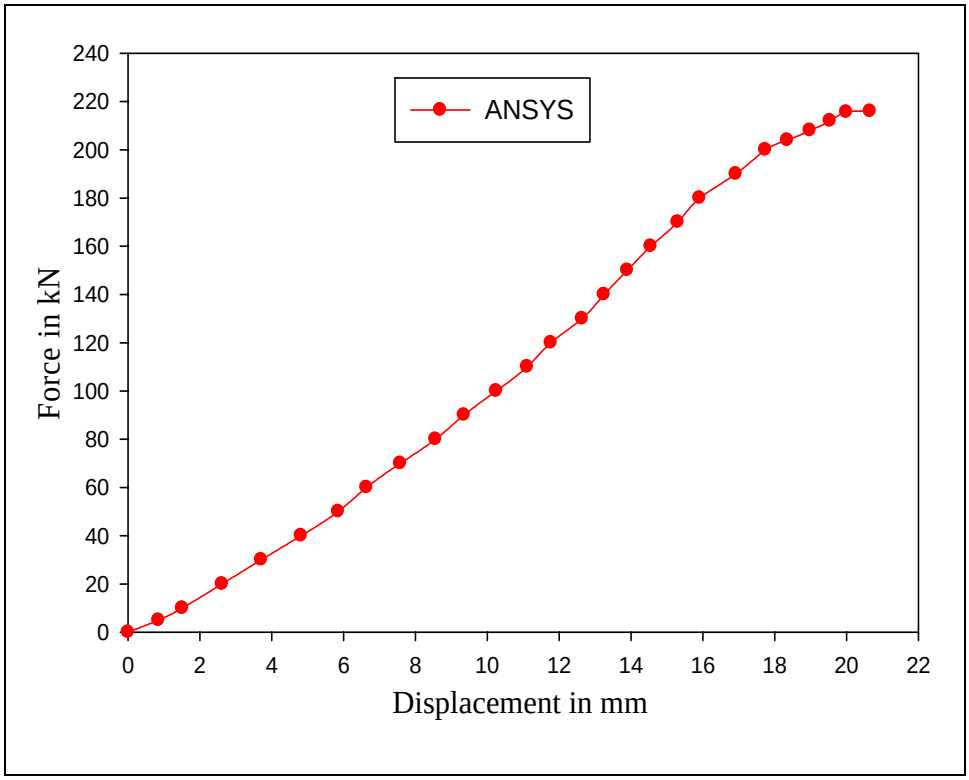

Fig. 4.14: Graph between force and displacement for specimen WT 6

4.3 RESULTS COMPARISON (EXPERIMENTAL Vs ANSYS)

The results obtained through ANSYS are then compared with the experimental ones. Fig. 4.15-4.26 shows the fair matching of the results.

- **SPECIMEN WT 1**:

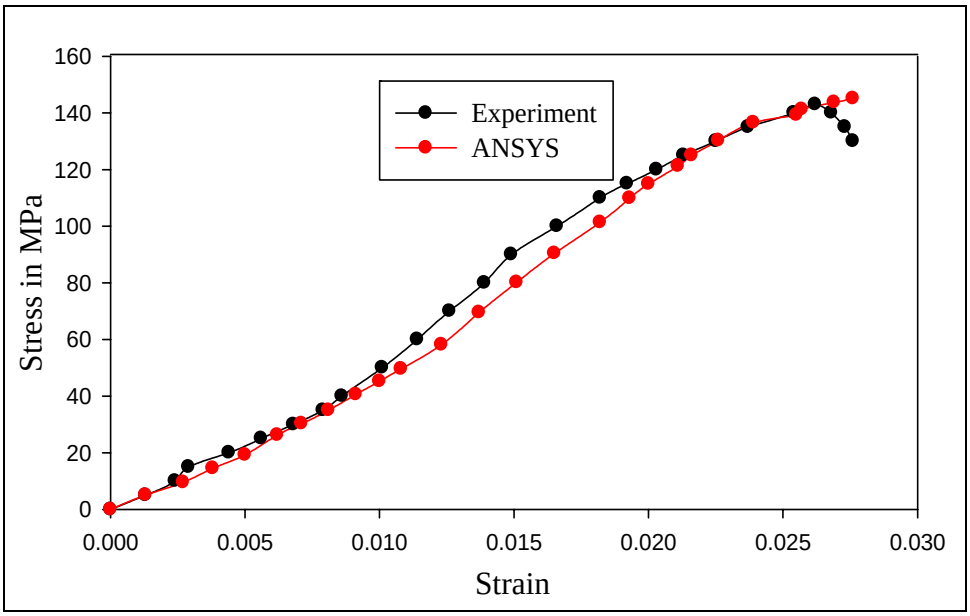

Fig. 4.15: Comparison of Experiment Vs ANSYS results for specimen WT 1 (Stress Vs strain)

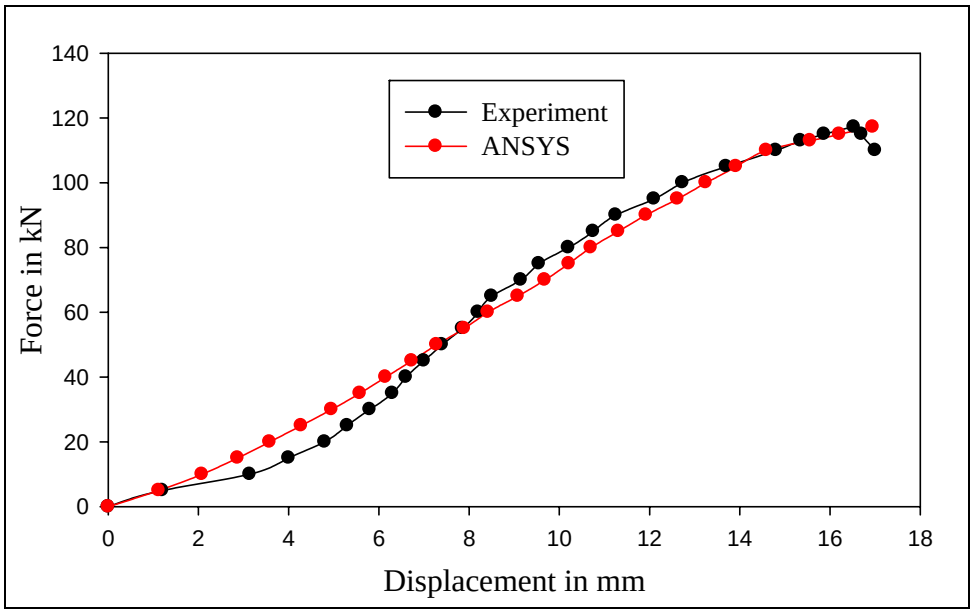

Fig. 4.16: Comparison of Experiment Vs ANSYS results for specimen WT 1 (Force Vs displacement)

- **SPECIMEN WT 2:**

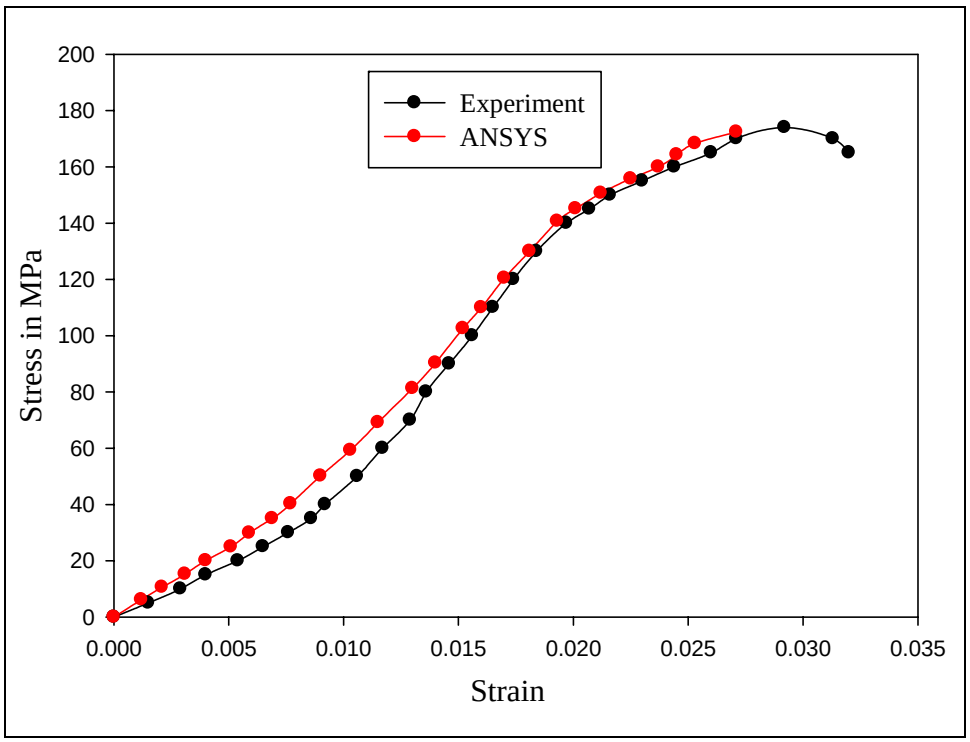

Fig. 4.17: Comparison of Experiment Vs ANSYS results for specimen WT 2 (Stress Vs strain)

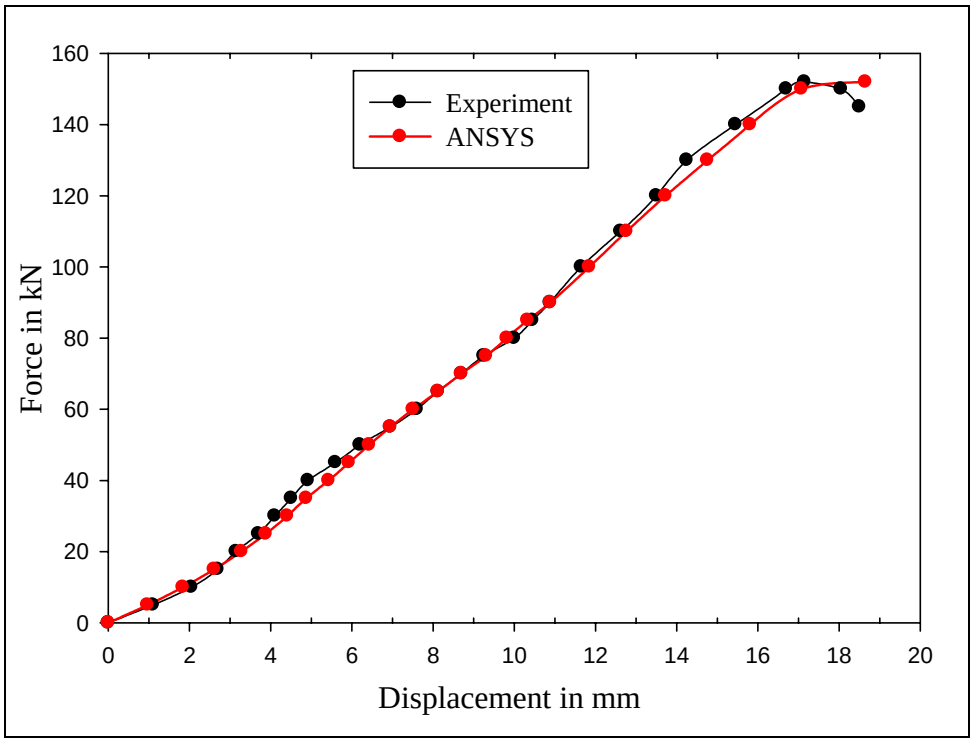

Fig. 4.18: Comparison of Experiment Vs ANSYS results for specimen WT 2 (Force Vs displacement)

- **SPECIMEN WT 3**:

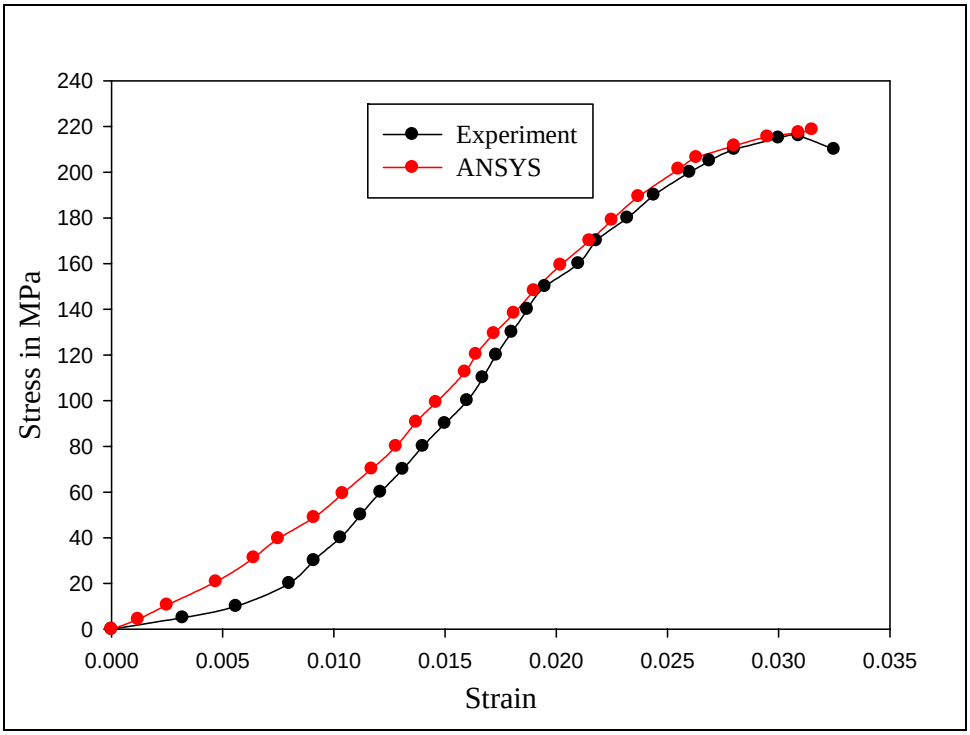

Fig. 4.19: Comparison of Experiment Vs ANSYS results for specimen WT 3 (Stress Vs strain)

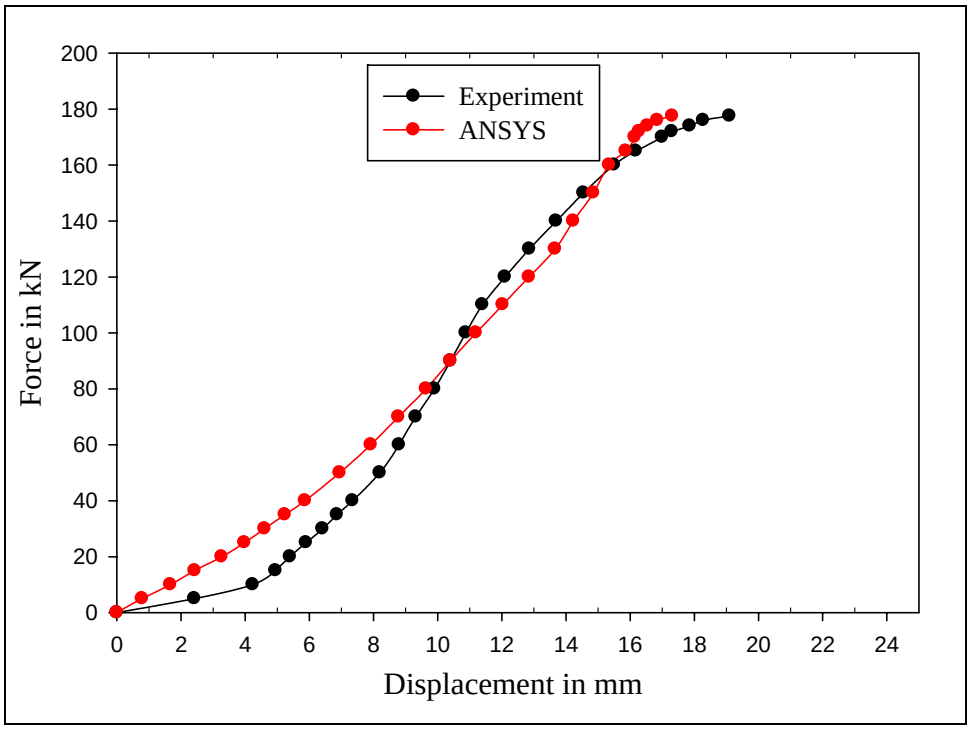

Fig. 4.20: Comparison of Experiment Vs ANSYS results for specimen WT 3 (Force Vs displacement)

- **SPECIMEN WT 4**:

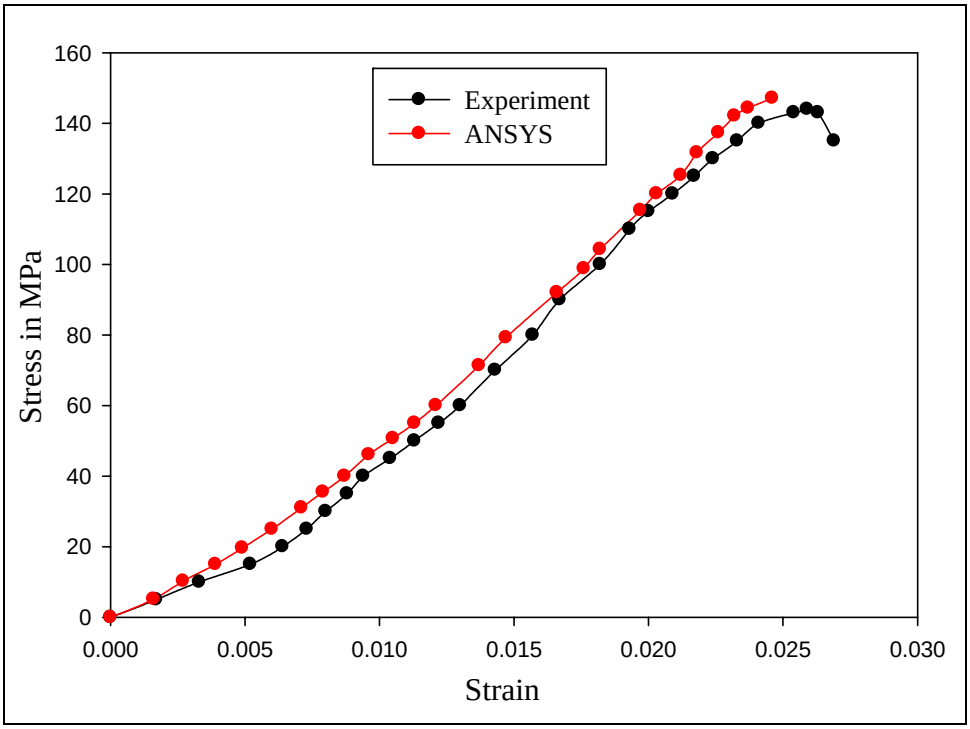

Fig. 4.21: Comparison of Experiment Vs ANSYS results for specimen WT 4 (Stress Vs strain)

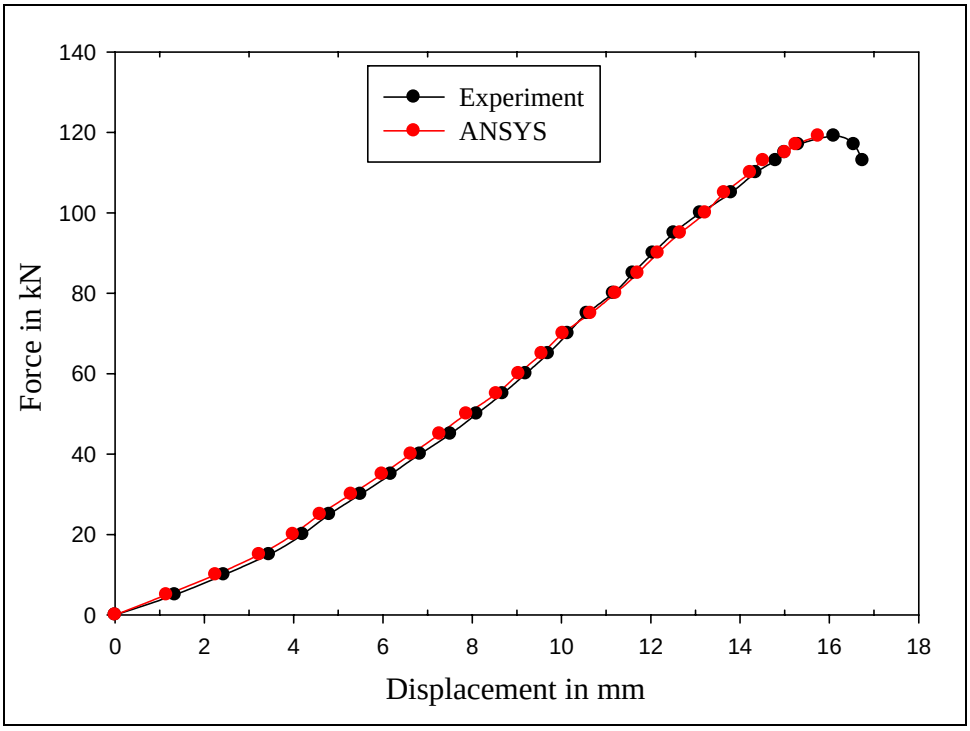

Fig. 4.22: Comparison of Experiment Vs ANSYS results for specimen WT 4 (Force Vs displacement)

- **SPECIMEN WT 5**:

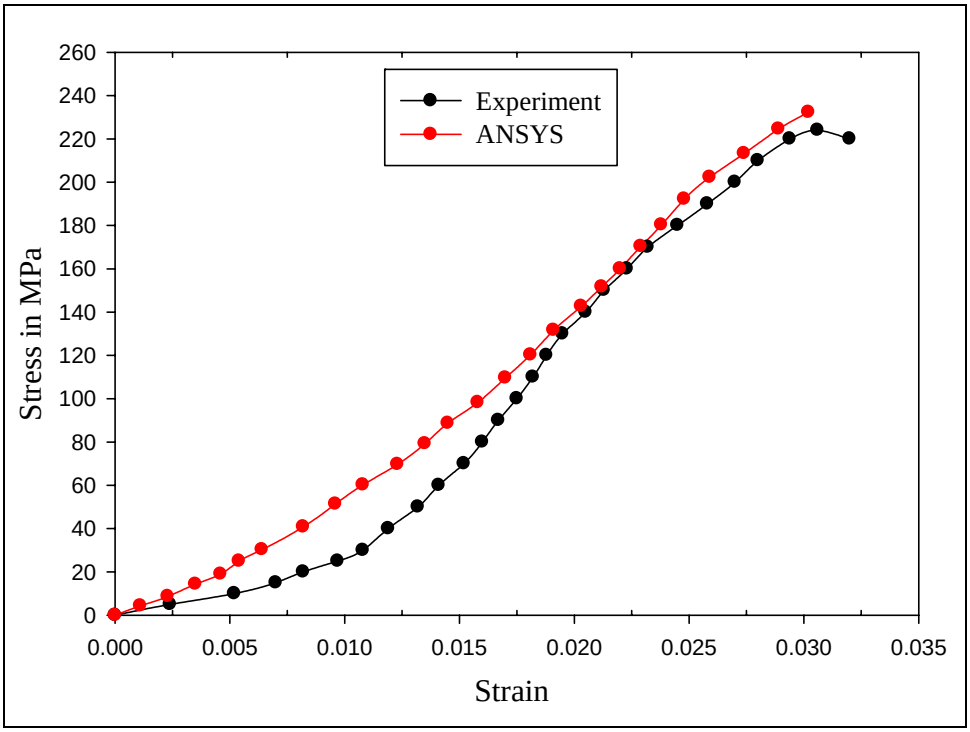

Fig. 4.23: Comparison of Experiment Vs ANSYS results for specimen WT 5 (Stress Vs strain)

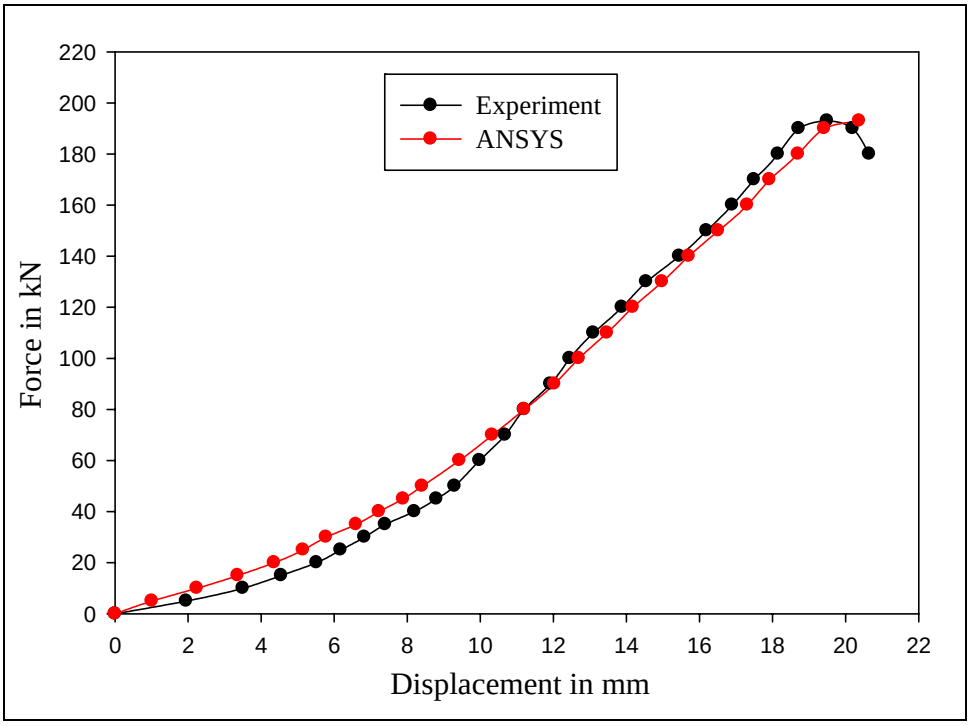

Fig. 4.24: Comparison of Experiment Vs ANSYS results for specimen WT 5 (Force Vs displacement)

- **SPECIMEN WT 6**:

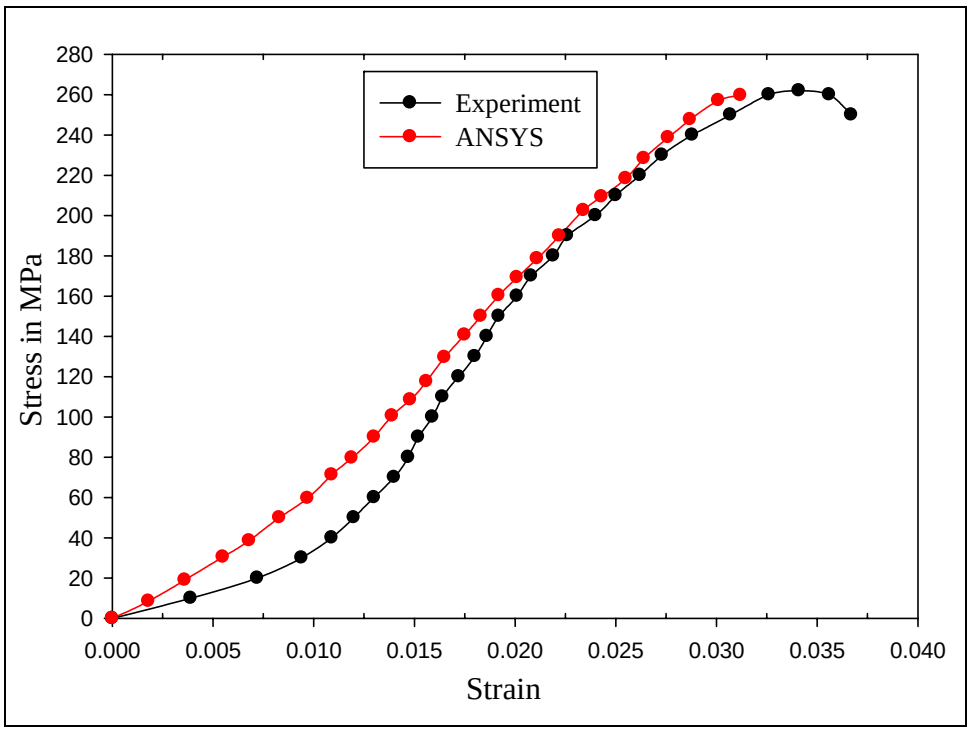

Fig. 4.25: Comparison of Experiment Vs ANSYS results for specimen WT 6 (Stress Vs strain)

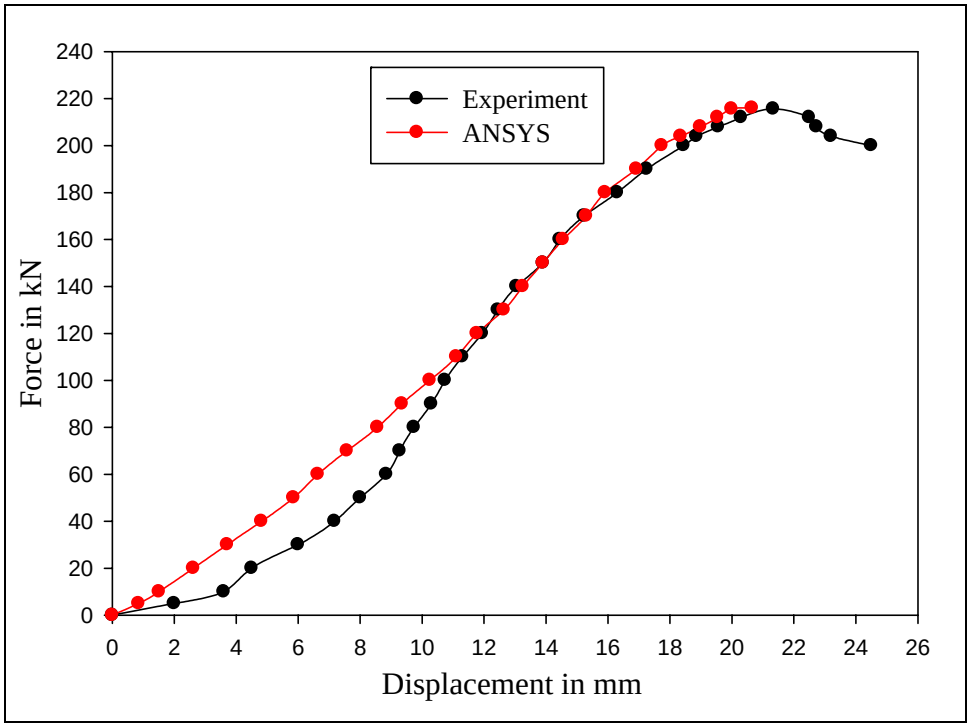

Fig. 4.26: Comparison of Experiment Vs ANSYS results for specimen WT 6 (Force Vs displacement)

CHAPTER 5
CONCLUSION AND SCOPE FOR FUTURE WORK

5.1 CONCLUSION

The study focused on examining the effect of varying connection eccentricity and connection length on the ultimate capacity of the bolted WT tension members. Here the connection length is increased by increasing the pitch between the holes instead of increasing the number of bolts as given by K. E. Barth *et al.* [9].

In all of the specimens, failure is caused due to the partial net section rupture of the connected leg adjacent to the lead bolt hole. The Finite Element Analysis presented here is capable of not only predicting the failure capacities but also in tracing the entire load versus deflection path.

The analysis indicated an excellent agreement with the experimental failure capacities of the specimens with large connection eccentricities. In addition, these models are able to accurately capture the partial net section rupture failure mode observed in the experimental specimens.

5.2 SCOPE FOR FUTURE WORK

1. The above work can be extended for different metals.
2. The work can be extended for specimen with the punched hole instead of drilled hole as in present work.
3. Higher order element can be used to get more precise results.

REFERENCES

[1] W. H. Munse and J. R. Chesson, "Riveted and bolted joints: net section design", *ASCE Journal of Structural Engineering*, vol. 89, No. ST1, pp. 107-126 (1963).

[2] J. M. Ricles and J. A. Yura, "Strength of double-row bolted-web connections", *ASCE Journal Struct Eng*, vol. 109, pp. 126–142 (1983).

[3] AISC. "Allowable stress design and plastic design specifications for structural steel buildings", 9th ed. Chicago (IL), *American Institute of Steel Construction*, 1989.

[4] AISC, "Load and resistance factor design specifications for structural steel building", 2nd ed. Chicago (IL), *American Institute of Steel Construction*, 1995.

[5] J. M. Gross, J. G. Orbison and R. D. Ziemian, "Block shear tests in high strength steel angles", *AISC Engineering Journal*, vol. 32 (3), pp. 117-122 (1995).

[6] H. I. Epstein and R. Chamarajanagar, "Finite Element studies for correlation with block shear tests", *Comput Struct*, vol. 61, pp. 967–974 (1996).

[7] G. L. Kulak and E. Y. Wu, "Shear lag in bolted angle tension members", *ASCE Journal Struct Eng*, vol. 123 (9), pp.1144–1152 (1997).

[8] J. G., Orbison, M. E Wagner and W. P. Fritz, "Tension plane behavior in single-Row bolted connections subject to block shear", *Journal of Constructional Steel Research*, vol. 49, pp. 2-15 (1999).

[9] K. E. Barth, J. G. Orbison and R. Nukala, "Behavior of steel tension members subjected to uniaxial loading", *Journal of Constructional Steel Research*, vol. 58, pp. 1103–1120 (2002).

[10] M. Gupta and L. M. Gupta, “Evaluation of stress distribution in bolted steel angles under tension”, *Electronic Journal of Structural Engineering*, vol. 4, pp. 17-27 (2004).

[11] C. L. Pan, “Prediction of the strength of bolted cold-formed channel sections in tension”, *Journal of Thin-Walled Structures*, vol. 42, pp. 1177–1198 (2004).

[12] C. Topkaya, “Finite element parametric studies on block shear failure of steel tension members”, *Journal of Constructional Steel Research*, vol. 64 (11), pp.1615–1635 (2004).

[13] C. H. Michael, Y. C. Yama, Zhongb, C. C. Angus, Lamb and V. P. Iub, “An investigation of the block shear strength of coped beams with a welded clip angle connection—Part I: Experimental study”, *Journal of Constructional Steel Research*, vol. 63, pp. 96–115 (2007).

[14] C. H. Michael, Y. C. Yama, Zhongb, C.C. Angus, Lamb and V. P. Iub, “An investigation of the block shear strength of coped beams with a welded clip angle connection—Part II: Numerical study”, *Journal of Constructional Steel Research*, vol. 63, pp. 116-134 (2007).

[15] V. F. de Paulaa, L. M. Bezerrab, and W. T. Matiasb, “Efficiency reduction due to shear lag on bolted cold-formed steel angles”, *Journal of Constructional Steel Research*, vol. 64, pp. 571–583 (2008).

[16] A. Bouchair, J. Averseng and A. Abidelah, “Analysis of the behaviour of stainless steel bolted connections”, *Journal of Constructional Steel Research*, vol. 64, pp. 1264–1274 (2008).

[17] T. Ranawaka and M. Mahendran, “Experimental study of the mechanical properties of light gauge cold-formed steels at elevated temperatures”, *Fire Safety Journal*, vol. 44, pp. 219-229 (2008).

[18] T.N. Chakherlou, R.H. Oskouei and J. Vogwell, “Experimental and numerical investigation of the effect of clamping force on the fatigue behaviour of bolted plates”, *Engineering Failure Analysis*, vol. 15, pp. 563–574 (2008).

BIBLIOGRAPHY

[1] M. J. Turner, R. W. Clough, H. C. Martin and L. J. Topp, " Stiffness and deflection analysis of complex structures", *Journal of the Aeronautical Sciences* vol. 23, pp**.** 805–823 (1956).

[2] E. H. Gaylord, C. N. Gaylord and J. E. Stallmeyer, "Design of steel structures", McGraw-Hill Publication, New York, 1992.

[3] J. N. Reddy, "Introduction to the Finite Element Method", McGraw-Hill International Editions, London, 1993.

[4] R. Tirupathi Chandrupatla and D. Ashok Belegundu, "Introduction to Finite Elements in Engineering", Prentice Hall of India Pvt. Ltd., New Delhi, 1997.

[5] O. C. Zienkiewicz, "The Finite Element Method", Tata McGraw-Hill Publication, London, 2003.

[6] David V. Hutton, "Fundamental of Finite Element Analysis", McGraw-Hill International Editions, London, 2004.

[7] J. N. Reddy, "An Introduction to the Nonlinear Finite Element Analysis", Oxford University Press, London, 2004.

[8] Rajneesh Joshi, "Non Linear Analysis of Tensile Test using Finite Element Method", M.E. Thesis, Mechanical Engineering Department, Thapar University, Patiala, (2007).